

A Dissertation On

COMPARATIVE ANALYSIS OF DECAY
PROCESSES IN
 $^{20}\text{Ne} + ^{181}\text{Ta} \rightarrow ^{201}\text{Bi}$ REACTION

Dissertation submitted in partial fulfillment for the requirement of
The award of the degree of
Masters of Science
In
PHYSICS

Under
The supervision of
Dr. Manoj K. Sharma

Submitted by
Gurvinder Kaur
Roll no. :- 300804009



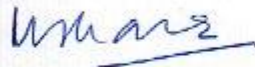
School of Physics and Materials Science
Thapar University
Patiala-147004, INDIA
June, 2010

*Dedicated to My Family Members
Mentors and My Friends.*

CERTIFICATE

This is to certify that this thesis entitled "Comparative analysis of decay processes in $^{20}\text{Ne} + ^{181}\text{Ta} \rightarrow ^{201}\text{Bi}$ Reaction" is being submitted by Ms. Gurvinder Kaur, Roll no. 300804009 for the fulfillment of the award of Degree of Masters of Science in Physics in the School of Physics And Material Science (SPMS), Thapar University, Patiala, is a record of candidate's own work carried out under our supervision. The matter presented in this thesis has not been submitted in part or full for the award of any degree in any other University or Institute.

Supervisor



(Dr. Manoj K. Sharma)
Associate Professor
SPMS, Thapar University
Patiala

Countersigned by:



Dr. O.P. Pandey
(Prof. and Head)
SPMS, Thapar University.
Patiala-147 001



Dr. R.K. Sharma
Dean of academic affairs
Thapar University
Patiala

ACKNOWLEDGEMENTS

In the first place, the author record her profound gratitude to her M.Sc. thesis supervisor Dr. Manoj K. Sharma, Associate Professor, School of Physics and Materials Science, Thapar University, Patiala, for their illuminating guidance and unflinching encouragement to complete this thesis work successfully. Dr. Manoj K. Sharma's constant support, dynamic supervision, valuable and innovative suggestions enabled the author to carry out this work effectively. It is a fortune for the author for being associated with him.

The author offers her special thanks to Prof. O.P. Pandey, Head School of Physics and Materials Science, Thapar University, Patiala, for providing all the necessary facilities in the department. Also, the author wishes to express his thankfulness to all the faculty and staff of the School for their kind support. The author is thankful to Prof. K.K. Raina, Deputy Director, and Prof. N.K. Verma, Dean Student Welfare, for their encouragement and constant moral support to accomplish this task.

Thanks will not be complete if author does not mention the names of Mrs. Shefali Kanwar, Miss Gudween sawhny and Miss Manpreet kaur the doctoral scholars of School of Physics and Materials Science, Thapar University, Patiala for their support.

Most importantly, the author is indebted to her parents who worked industriously to support the family without complaining, in spite of hardships and spared no effort to provide the best possible environment for her to achieve this target. This work is dedicated to her parents (S.Ranjit Singh and Mrs. Sukhvinder Kaur) and her brother for their love and sacrifice. Special thanks are reserved for her ever cheerful friends because without their loving and caring attitude throughout, the life would not be so active and good.

The author feels that the chain of gratitude would be definitely incomplete without thanking the Almighty, the prime mover, for inspiring and guiding her (the humble being) to complete this task successfully.

Patiala,
July 2010

Gurvinder Kaur.

Contents

Page No.

Abstract.....	7
---------------	---

1. Introduction

1.1	Introduction.....	8
1.2	Heavy ion nuclear reactions.....	8
1.3	Compound nuclear reactions.....	9
1.4	Compound nucleus(CN).....	10
1.5	Nuclear fission.....	12
1.6	Nuclear fusion.....	15
1.7	Importance of fusion-fission reactions.....	16
1.8	Fusion hindrance.....	18
1.9	Incomplete fusion (ICF).....	18
1.10	Influence of ICF on complete fusion.....	19
1.11	Fractional linear momentum transfer in ICF.....	19
1.12	Deep inelastic collision (DIC).....	21
1.13	Quasi-fission(QF).....	22
1.14	Quasi-fission and fusion.....	24
	References.....	24

2. Methodology

2.1	Introduction.....	27
2.2	The Scattering Potential.....	29
2.3	Fragmentation Potential.....	30
2.4	Proximity Potential.....	31
2.5	Coulomb Potential.....	32
2.6	Quantum Mechanical Fragmentation Theory.....	33
2.7	Prefromation Probability.....	35
2.8	Penetration Probability.....	36
2.9	Assault Frequency.....	36
	References.....	37

3. Results for Decay of ^{201}Bi

3.1	Introduction.....	40
3.2	Results and discussion.....	41
3.3	Referances.....	50

List of Figures

- Fig 1.1 Nuclear levels in a compound nucleus
- Fig.1.2 Time scales of compound nucleus
- Fig.1.3 Fission product
- Fig 1.4 Percentage non-compound nucleus contribution
- Fig 1.5 Variation of fractional ICF
- Fig 1.6 Complete fusion and ICF results
- Fig 1.7 Dynamics of colliding nuclei
- Fig 2.1 Scattering Plot for $^{20}\text{Ne}_{10} + ^{181}\text{Ta}_{73} \rightarrow ^{201}\text{Bi}_{83}$
- Fig 3.1 Variation of σ_{LP} as a function of angular momentum $\Delta R_{ER}=1.246$ fm
- Fig 3.2 Graph for preformation probability at $\Delta R_{ER}=1.246$ fm
- Fig 3.3 Scattering plot for $^{20}\text{Ne} + ^{181}\text{Ta} \rightarrow \text{Bi}^{201}$ reaction $\Delta R_{fission}=1.750$ fm
- Fig 3.4 Graph for maximum angular momentum for $\Delta R_{fission}=1.750$ fm
- Fig 3.5 Variation of Preformation probability with mass number $\Delta R_{fission}=1.750$
- Fig 3.6 Fragmentation potential at I_{Max} for two different ΔR values
- Fig.3.7 Graph for preformation probability for $\Delta R_{ER}=1.708$ fm
- Fig. 3.8 Graph for preformation probability $\Delta R_{fission}=2.000$ fm
- Fig 3.9 Scatering plots for both deformed and spherical fragments

ABSTRACT

The collision between a heavy ion projectile and a target nucleus may lead to the formation of compound nucleus (CN) as well as non-compound nucleus (NCN). Hence it can not be directly concluded that in what manner the final products of a nuclear reaction would be formed. In addition to this fact another thing worth noting is that we also can't easily get an idea of the decay process(es) involved in a reaction i.e. whether the system which we have obtained from the reactants decays giving compound nucleus contribution or it decays giving Non-Compound Nucleus(NCN) contribution. Not only this, another case is where the decay can be from CN nucleus as well as NCN simultaneously for a single system under consideration. Measurement of fission products and evaporation residues in general provide a comprehensive picture of the process subsequent to collision between projectile and target nucleus. In order to investigate various decay mechanisms in $^{20}\text{Ne}_{10} + ^{181}\text{Ta}_{73}$ reaction forming $^{201}\text{Bi}_{83}$ system, the ER, fission cross-section data obtained from experimental results have been studied. In order to have detailed knowledge of the changes that may occur when the deformation effects are included the given system i.e. ^{201}Bi has been studied explicitly for the deformed and spherical cases. The theoretical study of the decay of ^{201}Bi system through DCM model for deformed case gave the information that reported cross-section of the lighter particles is similar as that of the theoretically calculated one. But, the fission cross-section support the idea of contribution from NCN channel as the value for it could not match with reported value. Further the spherical case also revealed the similar results except for the fact that the expected contribution from NCN comes out to be more than that from the deformed case.

Chapter – 1

INTRODUCTION

1.1 Introduction

Understanding the fundamental nature of matter was an exclusive pursuit of scientists for a long time, almost two hundred years ago. It got great impetus, with the pioneering discoveries of electron during the last decade of 19th century. Since then the microscopic world of atomic nucleus has been explored intensively. This study is named as nuclear physics. In an atom, nucleus is very small, dense region, sitting at its centre, consisting of nucleons (protons and neutrons). The nucleus is a little, positive center that makes up very little of the actual atom but plays an instrumental role in its properties and applications. It is quite an interesting story as to how the atomic nucleus was first discovered, by E. Rutherford in 1911, and perceived. Just as close connection between theory and experiment had proved fruitful for atomic physics, the same connection comes to work well in the study of nucleus. This can be supported from the fact that as the German physicist Otto Hahn and Fritzstrtsman in 1938 had made the unexpected and unexplained discovery that uranium atom can be split in two approximately equal halves, when bombarded with neutrons. No sooner, in the beginning of 1939, in United States a fierce race to confirm experimentally the so-called fission of the nucleus began after the news of the German experiments and their explanation had become known. Finally it was Bohr who did the path breaking work with his younger American colleague John Archibald Wheeler at Princeton University to explain fission theoretically. The consistent efforts on the experimental and theoretical fronts finally led to the current understanding of a nucleus and the atom. Over the years, in order to keep pace with the rapid accumulation of experimental data, nuclear models are being developed and have become integral part in the development of nuclear physics.

1.2 Heavy Ion Nuclear Reactions

A nuclear reaction is described by identifying incident particle/nucleus with specific associated incident energy, target nucleus, and reaction products. In order for a nuclear reaction to occur, the nucleons in the incident particle or projectile must interact with the nucleon in the target. Thus the energy must be high enough to overcome the natural electromagnetic repulsion between the protons. This energy barrier is called "Coulomb barrier". The demarcation of energy is done through this barrier. If the energy is below the barrier, the nuclei will bounce off each other. Since the first experimental demonstration of nuclear reaction process by Rutherford in 1919, experimental techniques in the field of nuclear physics have improved immensely. Formerly, in the study of nuclear reactions projectiles used were basically the alpha particles from natural radioactive substances. Also, the discovery of neutron in 1932 caused an impetus in the nuclear reaction experiments. Low energy neutrons can easily penetrate Coulomb barrier and cause nuclear reactions. Later on, the advent of highly advanced particle accelerators techniques have made possible high

energy beams of not only protons, deuterons and alpha particles but also heavy ions, to produce nuclear reactions. Highly efficient and precise detector technology, to observe nuclear phenomena, is available. Fast computational methods further aided in precise and accurate measurements of cross sections and angular distribution of the disintegration products in the experiments. As a result, lot of experimental data related to different nuclear phenomena have become available.

Nuclear reactions induced by heavy ions have become the principal tool in nuclear physics research. They are used to measure the properties of nuclear forces and related aspects. Reactions that exchange energy or nucleons are helpful in finding the binding and excitation energies, quantum numbers of energy levels and transition rates between levels. The nuclear reactions can also be categorized on the basis of energy of projectiles, as low, intermediate and high energy reactions. Projectiles with energies < 10 MeV/nucleon and >400 MeV/nucleon cause low and high energy nuclear reactions respectively. Whereas the in between energy range corresponds to the intermediate energy reactions. In low energy reactions average/mean nuclear force field acting between the two nuclei dominate in comparison to high energy reactions where direct nucleon-nucleon interactions takes place. In intermediate energy reactions both the aspects play their role. However, in the present study we have confined ourselves to low energy nuclear reaction dynamics only. The present state of art experimental facilities lead to better understanding of nuclear forces with formation of heavy nuclei away from valley of stability. Moreover, one can explore various aspects of nuclear structure and dynamics "at extremes" and thus gain a deeper insight via study of decay products of Compound Nucleus formed in low energy nuclear reactions. There are many types of nuclear reactions but they may be divided roughly into two groups called

1. Compound nuclear reaction
2. Direct reaction

1.3 Compound Nuclear Reaction:-

In this group the bombarding particle is captured by the target nucleus to form an intermediate state-The COMPOUND NUCLEUS. The subsequent decay of this intermediate state is largely independent of mode of formation. Thus a given compound nucleus may be formed by different reactions but the probability of a certain type of final state is only dependent upon amount of excitation energy. The most obvious evidence for long lived intermediate state in nuclear reaction is the strongly resonant nature of nuclear cross- section. Listing all types of nuclear reactions in table 1.1

Table1.1. Showing various types of reactions and information provided by them.

S.No.	Nuclear reaction	Information obtained
1.	Nucleon- nucleon scattering	Fundamental nuclear force
2.	Elastic scattering of nuclei	Nuclear size and interaction

		potential
3.	Inelastic scattering to excited states	Energy level location and quantum numbers
4.	Inelastic scattering to the continuum	Giant resonances (vibrational modes)
5.	Fusion reactions	Astrophysical processes
6.	Fission reaction	Properties of liquid drop model
7.	Compound nuclear formation	Statistical properties of the nucleus

In broad terms nuclear reactions can be categorized into two types, namely Fusion reactions and Fusion-Fission reactions. These two processes play an important role in the production of new elements, their further studies and applications, etc. For successful formation of heavy nuclei, deep understanding of fusion-fission process of the compound nucleus formed in heavy ion reaction is essential. Hence, before talking explicitly about few of the above mentioned compound nuclear reactions we need to have an insight of the formation of Compound Nucleus(CN) , as well as its existence

1.4 Compound Nucleus (CN)

In an atomic nucleus, neutrons (neutral particles) and protons (positively charged particles) are held together by a strong nuclear force. Though information on exact nature of this force is still limited and not established analytically, like for the Coulomb force, much progress has been made towards its phenomenological understanding.

CN formation is a reaction in which two nuclei combine into a single excited nucleus, this excited nucleus lives for a relatively long time and “forgets“ how it was formed. In a compound nucleus its observed that for a short range or abrupt sided potential there exist quasi-bound or virtual single particle states which have positive energy. A long range potential like the coulomb potential has no such states. The positive energy projectile particle is momentarily trapped in one of the single particle virtual states. Through collision with nucleons inside the nucleus it shares its energy with them, raising some of them into excited states and itself dropping into one of these states by virtue of the energy it loses. This is the formation of the many particle excited state which is the compound nucleus. At this stage all memory of the original mode of excitation is lost.

At a later time a decay possibility occurs when the energy of excitation is once more concentrated in a single or few particle virtual state. In the evolution of the many particle excited states several such fleeting decay configurations may occur before one of them is realized and the products separate out. A CN is observed to undergo two different kinds of processes:-

(a) It subsequently decays by emission of particles and γ -ray to form evaporation residues.

(b) It may undergo fission if excitation energy is higher than fission barrier.

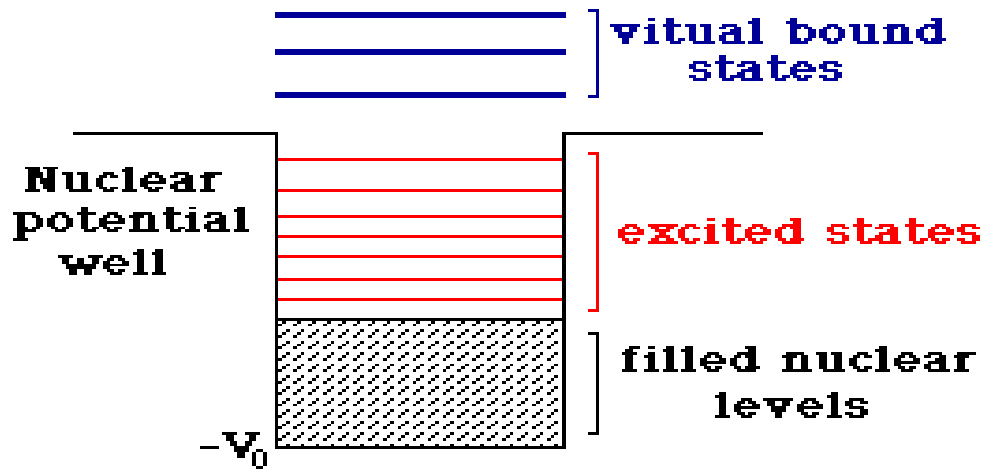


Fig.1.1 Nuclear levels in a compound nucleus

The statistical nature of the process teaches us about the average properties of excited state of complex nuclei. The energy of these long-lived states is defined to a few eV and if we apply the uncertainty relation $dE \cdot dt \sim \hbar$ we can see that this implies a lifetime of 10^{-16} s which is very long compared to the time a nucleon takes to transverse a nucleus $\sim 10^{-22}$ s. The time scale of the order of 10^{-22} sec, can be measured through neutron clock. A method in which the number of neutrons emitted prior to fission are counted as an indicator of how much time has passed before the fission takes place. These measurements demonstrate that fission is a slow process (about 50-100 times slower) as compared to the expected time scale. These measurements are indicative of the time taken for the nucleus to “re-arrange” itself in preparation to dividing into two smaller pieces. In a heavy-ion reaction there is also a considerable formation time (time for the projectile to get assimilated with the target to form the compound nucleus). The compound nuclei (CN) formed in low-energy heavy-ion reactions are highly excited and carry large angular momentum. The compound systems so formed decay by emitting multiple light particles, LPs (n, p, α) and γ -rays.

For light compound systems with $A_{CN} \gg 40 - 80$, the light-particles (LPs) emission is always accompanied by intermediate mass fragments, the IMFs (with $2 < Z < 10$ and $5 < A < 20$). In this mass region the IMFs contribution is very small of the order of 5-10%, in comparison to LPs contribution. However, for the heavy nuclear systems $A_{CN} \ll 200$, the most probable decay mode of the compound nucleus is fission/ heavy mass fragments (HMFs) ($20 < A < A/2$), due to its instability against centrifugal repulsion, with small contribution from neutrons and γ -rays emissions, just in contrast to decay process of light compound systems.

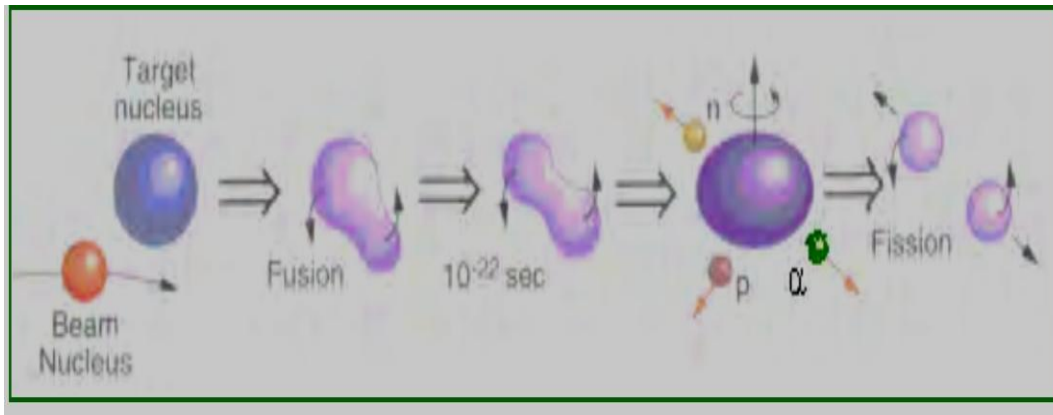


Fig.1.2 Time scale of compound nucleus

Then there are other processes which may contribute to decay products, e.g., orbiting, deep-inelastic and quasi-fission, etc., depending upon the reaction conditions. After gaining this information regarding compound nucleus we can surely move ahead discussing two of the compound nuclear reactions- the fission and the fusion reactions.

1.5 Nuclear Fission

One of the most interesting phenomena in Nuclear Physics with far reaching consequences is the fission of atomic nuclei.

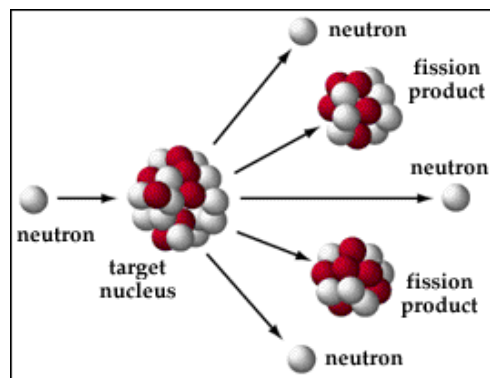


Fig. 1.3 Neutron strikes the target nucleus to give fission product

It is the Division of a heavy atomic nucleus into two fragments of roughly equal mass, accompanied by the release of a large amount of energy which is the binding energy of the subatomic particles. The sum of the masses of these fragments is less than the original mass. This 'missing' mass (about 0.1 percent of the original mass) has been converted into energy according to Einstein's equation. Fission can occur when a nucleus of a heavy atom captures a neutron, or it can happen spontaneously.

The energy released in the fission of one uranium nucleus is about 50 million times greater than that released when a carbon atom combines with oxygen atoms in the burning of coal. The energy appears as kinetic energy of the fragments, which converts to thermal energy as the fragments collide in matter and slow down.

Fission also releases two or three free neutrons. The free neutrons can bombard other nuclei, leading to a series of fissions called a chain reaction. An interesting thing to be noticed is that when a slow moving neutron strikes a heavy nucleus like Uranium it breaks up into two fission fragments. The puzzling feature of this nuclear reaction is how a nucleus consisting of more than 200 protons and neutrons could split into two pieces with so little provocation. This is analogous to breaking a huge rock by a feather touch. The answer was given by Neils Bohr in 1939, in his theory where he likened the nucleus to a liquid drop. While the Bohr-Wheeler theory touched the essence of the fission problem, modern research shows that the vibrating nucleus behaves more like a drop of honey rather than a drop of water. These developments came about as the scientists began measuring fission time scales.

Nuclear fission has been exhaustively studied in past few decades and a large amount of experimental data for various vibrating systems has been generated. A light nucleus can contain hundreds of nucleons and with some approximations it can be treated as a classical system, rather than a quantum-mechanical one, resulting into the liquid-drop model (macroscopic approach). It is assumed that the nucleus has an energy which arises partly from surface tension and partly from electrical repulsion of the protons. This model is able to reproduce many features of nuclei, including the general trend of binding energy per nucleon with respect to mass number, as well as the phenomenon of nuclear fission and fusion. Heavy ions (HI) have been used increasingly as projectiles to study the fission of CN for a wide range of fissility Z^2/A , excitation energy and angular momentum. Studies on the effect of these parameters on various fission observables have provided deeper insights into the mechanisms of fission. Apart from this it has also been possible to study mechanisms of HI reaction such as transfer reaction and various other NCN processes through fission observables.

In general, the HI induced fission reactions, fission events consist of an admixture of events of 2 types

- Fission following the formation of fully equilibrated CN which relaxes in all degrees of freedom.
- Fission of a NCN which is composite system which has equilibrated in all degrees of freedom except K degree of freedom, where K is projection of angular momentum (J) on the symmetry axis identified as fission axis.

The formation of compound nucleus – the complete fusion and the non compound nucleus- the incomplete fusion is governed by the angular momentum limitation in the entrance channel.

- The collision trajectories with $\ell < \ell_{\text{crit}}$ are trapped in the pocket in the entrance channel potential leading to fusion.
- On the other hand, for the collision trajectories with $\ell > \ell_{\text{crit}}$, pocket in the entrance channel potential vanishes, and therefore such trajectories will lead to non compound nucleus processes such as deep inelastic collisions (DIC) and incomplete fusion reaction (ICF).

Understanding the break-up mechanism and its impact on nuclear reaction dynamics is essential. A major consequence of break-up is that a rich scenario of reaction pathways arise such as events where

- Not all the resulting breakup fragments might be captured by the target, termed incomplete fusion (ICF),
- The entire projectile is captured by the target, called complete fusion (CF), and
- None of the breakup fragments are captured, termed no- capture breakup (NCBU).

Fission following the NCN formation may have contribution of large number of reaction mechanisms. These reaction mechanisms in collision between two nuclei mainly depend on the entrance channel parameter, namely beam energy and mass asymmetry. The mechanisms are:

- Fast Fission- Where we have composite system with zero fission barrier .
- Quasi- Fission- Having composite system with fission barrier shape more compact than entrance contact configuration
- Pre-equilibrium fission- Occurring in a time scale comparable to characteristic relaxation time in K degree of freedom when fission barrier height becomes comparable to the temperature of the composite system.
- Incomplete Fusion- It's observed in reaction involving highly fissile actinide as one of collision parameters.

The NCN processes mainly constitute transfer and ICF processes . While transfer reactions start occurring at beam energy around the coulomb barrier , the ICF reactions are expected to occur at beam energy where the pocket in the entrance channel interaction potential disappears. The contribution from NCN fission results in deviation of fission angular anisotropy from statistical theory calculation and suppression in formation of evaporation residue.

The relative probabilities of fission events following CN and NCN can be obtained by considering a fused composite system with angular momentum ℓ and temperature T. If ℓ is larger than rotational liquid drop model limit (RLDM) ℓ_{RLDM} for vanishing fission barrier, no compound nucleus will be formed and

composite system will undergo fast fission with unit probability. If ℓ is less than ℓ^{RLDM} , fission barrier height the $B_F(\ell, K = 0)$ is calculated first. The corresponding fission probability per unit time can then be obtained making use of the Bohr-Wheeler transition state theory [1]. Thus assumed that only those composite systems that survive fission for a time longer than the characteristic K equilibration time τ result in the formation of a fully equilibrated compound nucleus which subsequently undergoes fission, while all fission events taking place in a time less than τ carry a memory of the entrance channel K distribution and have angular distributions characteristic of the type (ii) events i.e. NCN type. [2].

One of the important observation in early studies was discovery of asymmetric mass distribution in low energy fission of majority of actinides. This was explained by incorporating shell correction to liquid drop model fission barrier. With increase in excitation energy E^* , asymmetry in mass distribution decreases and at higher excitation energy symmetric mass distribution is observed. This has been explained as a result of gradual decrease of shell effects with increasing excitation energy. Though combination of shell effect and liquid drop model can explain basic feature of nuclear fission, there are certain aspects that are far from being completely understood and hence nuclear fission continues to be an important area of research.

1.6 Nuclear fusion

Fusion is a process in which two nuclei are brought together to form a compound nucleus (CN). A substantial energy barrier, due to mutual repulsion between the two nuclei, opposes the fusion reaction. This barrier consists of the Coulomb and the nuclear potentials. However, the long range Coulomb repulsion between the nuclei is offset by stronger, but short range, attractive nuclear force. Then, the problem is to bring the nuclei sufficiently close so that the Coulomb barrier can be crossed over, say, via tunneling. Hence, the two nuclei are required to collide with sufficient kinetic energy to overcome their mutual electrostatic repulsion (or fusion threshold barrier) and subsequently to bring into effect the role of strong but short range attractive nuclear force. In other words, the simplest picture of fusion is that of quantum tunneling through a one dimensional barrier formed by the long range Coulomb potential, the centrifugal potential and the short range nuclear potential. It means that the knowledge of interaction potential, forming barrier, between two nuclei is extremely important in order to have a systematic study of a nuclear reaction. The mechanism of fusion of two heavy ions has been extensively investigated. The motivation for such studies is to understand the effect of entrance channel parameters, viz., energy, angular momentum and mass asymmetry, on the fusion process.

It has been observed that the favorable compact shape results more easily into CN rather than an elongated touching shape. Here, the favorable compact shape means that the distance between the mass centers of target-projectile at touching should be less than the distance of centers of the nascent fission fragments at the fission saddle point. Hence, the relative distance between the mass centers of two colliding nuclei, with respect to saddle point, affects the

fusion of heavy ions considerably. For a system with large Z_1Z_2 product the contact point usually exists outside the saddle point. But in the fusion of deformed and relatively oriented nuclei the scenario is changed as at touching the distance between mass centers of massive reactants rely on the orientation of the deformed nuclei. It means that the fusion reaction starting from compact touching point results in higher fusion probability than the fusion starting from distant touching point. Thus the fusion process is greatly affected by the relative orientations of the deformed nuclei.

In the static fusion model, fusion process is viewed as the problem of crossing the barrier in the one-dimensional interaction potential between the two heavy ions [3,4]. The inclusion of deformation and orientation effects of the colliding nuclei leads to lowering of its barrier height. This means that the interaction potential and hence the fusion cross sections are largely influenced by the nuclear structure effects of the target and projectile nuclei and their relative orientations. The collisions between deformed as well as oriented nuclei have been studied extensively to establish the effect of deformation and orientation on fusion reactions [5]-[13]. It is important to note that when deformed and oriented nuclei collide, the fusion barrier height varies leading to the barrier height distribution around the spherical Coulomb barrier. Fusion can be considered as the most dissipative of heavy ion reaction processes, where the initial relative kinetic energy and angular momentum of the projectile is converted into intrinsic excitation energy and angular momentum of the fused system. When two heavy nuclei approach each other to distances closer than certain critical value, all those l values for which there exists a pocket in the potential energy as a function of the distance of separation, the nuclei can fuse leading to a compound nucleus formation. The total fusion cross section is given by,

$$\sigma_{fus} = \sum_{l=0}^{l_{cr}} \sigma_l$$

However, identification of the fusion process with trapping of the composite system into the potential pocket becomes uncertain, when heavier projectiles are used and at higher bombarding energies. Even after being trapped, the composite system may evolve towards symmetric fragmentation, without forming a true compound nucleus (CN) instead forming non compound nucleus (NCN).

1.7 Importance of fusion-fission reaction:

It has been possible to explore and investigate the dynamics of large shape changes in nuclear system by studying fusion-fission reactions. Beyond this, these reactions also proved to be of great importance from point of understanding the stability and production of heavy nuclei for extending the periodic table.

These aspects of the compound and the non compound nucleus can further be supported through various studies. For example [14] in $^{16}\text{O} + ^{66}\text{Zn}$ and $^{37}\text{Cl} + ^{45}\text{Sc}$

reactions the comparison of experimental excitation functions with the theoretically calculated excitation functions of proton emission (pxn) products namely ^{79}Rb and ^{78}Rb revealed that the experimental cross-sections agree well with the calculated cross-sections in both the systems indicating that these ERs are formed purely by complete fusion of projectile and target.

The experimental cross-section of an emission channel (^{77}Kr) deviate from the calculated cross-section in the case of $^{16}\text{O} + ^{66}\text{Zn}$ while it is well-reproduced in the case of $^{37}\text{Cl} + ^{45}\text{Sc}$ system. The mismatch between the experimental and calculated excitation functions has been considered to be due to contribution of NCN process in those channels. The excess cross-sections over what is expected from the compound nucleus process has been computed for each channel, at each beam energy, to obtain an estimate of the total non-compound cross-section as a function of beam energy for both the systems. With the support of this example, talking about the contribution from NCN which may involve any of the processes such as DIC, ICF, QF etc., we can say that the %NCN cross-section gradually increases with beam energy for system $^{16}\text{O} + ^{66}\text{Zn}$, whereas it remains practically invariant for $^{37}\text{Cl} + ^{45}\text{Sc}$ system in the beam energy range studied[14].

This may be due to the fact that the transfer channels mainly contribute to NCN processes in $^{37}\text{Cl} + ^{45}\text{Sc}$ system, while for the system $^{16}\text{O} + ^{66}\text{Zn}$, incomplete fusion (ICF) processes, in the form of α and 2α emission channels are observed. The analysis of experimental fusion and NCN cross-section in terms of static fusion model as well as sum rule model have revealed that NCN processes start competing with complete fusion process at l -value much below the vanishing l -pocket for mass asymmetric entrance channel.[14]

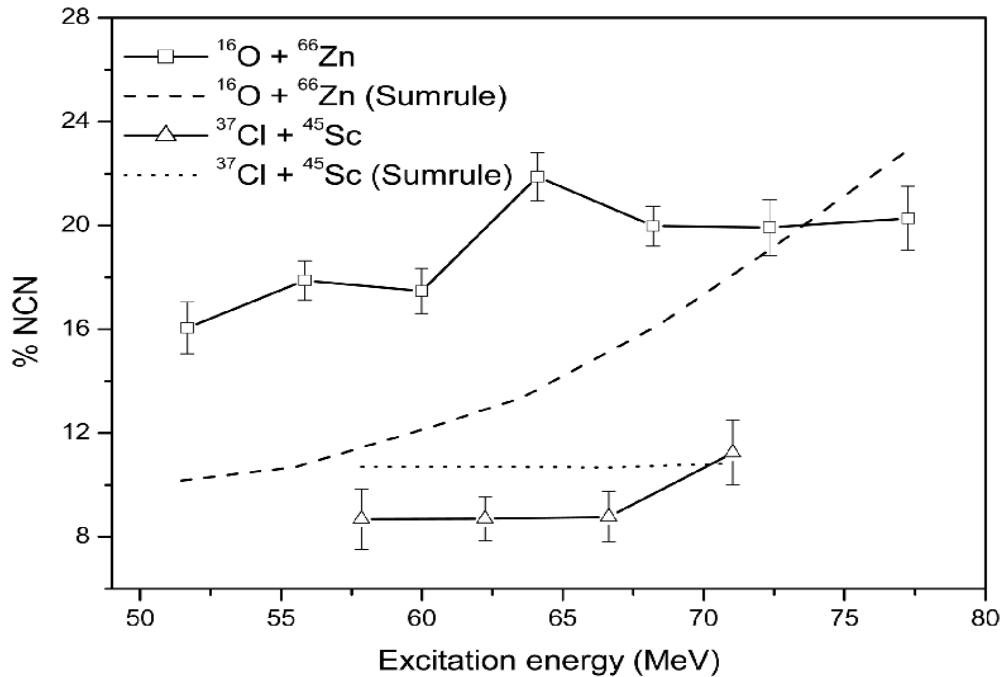


Figure 1.4 Percentage non-compound nucleus (NCN) processes in both the systems as a function of excitation energy[14].

1.8 Fusion Hindrance:

It is interesting to note that in the reaction of a heavy target-projectile combination, leading to heavier compound system, the crossing of a fusion barrier doesn't guarantee the formation of a CN. However, the system must overcome the saddle point of compound nucleus, which is located inside the fusion barrier between the heavy target and projectile. This hindrance in the fusion process is named as "extra-push" phenomenon and causes significant loss in the kinetic energy. Suppression in formation of evaporation residue, anomalous fission fragment angular distribution and broadening in fission fragment mass distribution are taken as signatures of fusion hindrance. Investigation of fusion hindrance requires measurement of fission fragment angular distribution and evaporation residue cross-sections in systems with varying entrance channel mass asymmetry.

Heavy ion fusion is not only affected by deformation and relative orientations of the reactants but also takes into account the nuclear shell structure of projectile and target nuclei. The shell closure of colliding nuclei plays a significant role in the sub-barrier fusion process [15], [16]. It indicates no fusion hindrance for the colliding nuclei with nuclear shell closure structure. The target and projectile with this type of structure makes a compact touching shape and produces an equilibrated compound nucleus.

Berriman et al [17] reported fusion hindrance based on the measurement of evaporation residue cross-section. Observation of fusion hindrance is attributed to the lower entrance channel mass asymmetry α_{BG} . (Businaro-Gallone critical mass asymmetry) However, fusion hindrance is observed to be much higher than that expected on the basis of pre-equilibrium fission model [18]. According to this model angular distribution is expected to deviate from the statistical theory for the reaction systems with $\alpha < \alpha_{BG}$. Measurement of fission fragment angular distribution shows that experimental anisotropies are consistent with statistical theory and significantly lower than those calculated using fusion suppression data from evaporation residue measurement. This disagreement indicate that result of measurement of fission fragment angular distribution and evaporation residue cross-section don't corroborate for reaction systems with small $Z_P Z_T$. [19] Studies of the interaction between heavy ion projectiles and heavy target nuclei have proven very useful in developing an understanding of the dynamics of nuclear matter at low energies. The outstanding characteristic of heavy ion collisions at energy close, and even below, the Coulomb barrier is the interplay between several channels (or several degrees) of freedom. A brief introduction of the various reaction mechanisms of the NCN has been mentioned in the previous section. Here we shall explain few amongst all those mechanisms which are most probable to occur so far as NCN is concerned. These mechanisms are ICF, DIC, QF.

1.9 Incomplete Fusion (ICF)

It can be explained to be a natural extension of fusion process for those collisions for which angular momentum limits the formation of complete fusion. The CF is said to occur when entire projectile fuses with target nucleus. While, only a part

of projectile fuses with target nucleus in case of ICF and unfused fragment continues to move in forward cone with almost projectile velocity. The linear momentum transfer in the ICF reaction is less than that in CF, resulting in lower range of the evaporation residue formed in the ICF reaction. In recent years, incomplete fusion (ICF) of light heavy ions ($A \leq 16$) has been intensively investigated at energies $\approx 4-7$ MeV/nucleon, where only complete fusion (CF) is supposed to be dominant. The main motivation of ICF studies is to explore the effect of various entrance channel parameters, such as;

- (i) Projectile energy,
- (ii) Mass-asymmetry of interacting partners, and
- (iii) Driving angular-momenta.

In addition to that, some outstanding issues related ICF are to examine the possibility to produce high spin states via ICF and the localization of ℓ -values. In view of the above issues, experiments have been performed to measure excitation functions (EFs), forward recoil ranges (FRRs), and spin-distributions (SDs) of heavy reaction products.

1.10 Influence of ICF on CF

It may be pointed out that, it is not possible to directly obtain the relative contributions of CF and ICF from the measurement of excitation functions (EFs). Therefore, indirect methods are used to deduce ICF contribution. In most of the α -emitting channels, a significant enhancement in the cross-sections over the theoretical predictions can be observed. Assuming this enhancement as a contribution of ICF (since PACE4 don't predict ICF), the percentage fractional ICF (F_{ICF}) can be deduced as a function of projectile energy and mass-asymmetry of interacting partners (Fig.1.5). In general, F_{ICF} increases with projectile energy for the given projectile target combination. The value of F_{ICF} also increases with mass-asymmetry. Therefore, it can be inferred that, not only mass-asymmetry of interacting partners but also the projectile structure effect should be taken into account while predicting the F_{ICF} .

1.11 Fractional linear momentum transfer in ICF

Kinematically, CF and ICF products can be disentangled on the basis of recoil velocity of the reaction products, depending upon the degree of linear momentum transfer (ρ_{LMT}) from projectile to the target nucleus. For ICF, ρ_{LMT} may be given as,

$$\rho_{LMT} = \frac{P_{frac}}{P_{proj}}$$

Where P_{frac} is the linear momentum of fused fraction of projectile and P_{proj} is the full linear momentum of projectile. Maximum ρ_{LMT} in CF is supposed to give maximum recoil velocity to the reaction products, and relatively less recoil velocity in ICF. Consequently, the radio-nuclides populated via small ρ_{LMT} (ICF products) are expected to show relatively smaller absorption depth in the stopping medium as compared to the entire LMT populations (CF products). The

profile of FRRs can be resolved into two Gaussian peaks figure 1.6 (a) revealing the presence of more than one LMT components. On the basis of observed most probable range (R_p), it can be inferred that the residues ^{181}Re produced via α emitting channel have contributions from both CF and ICF processes. This implies fractional momentum transfer in ICF. Fig.1.6 (b) shows, the relative contributions of CF and ICF in the production of ^{181}Re (α or $2p2n$) at $\approx 76, 81, 87$ MeV. The CF (fusion of ^{16}O) contribution decreases with projectile energy, while the ICF (fusion of ^{12}C) contribution is found to increase with projectile energy.

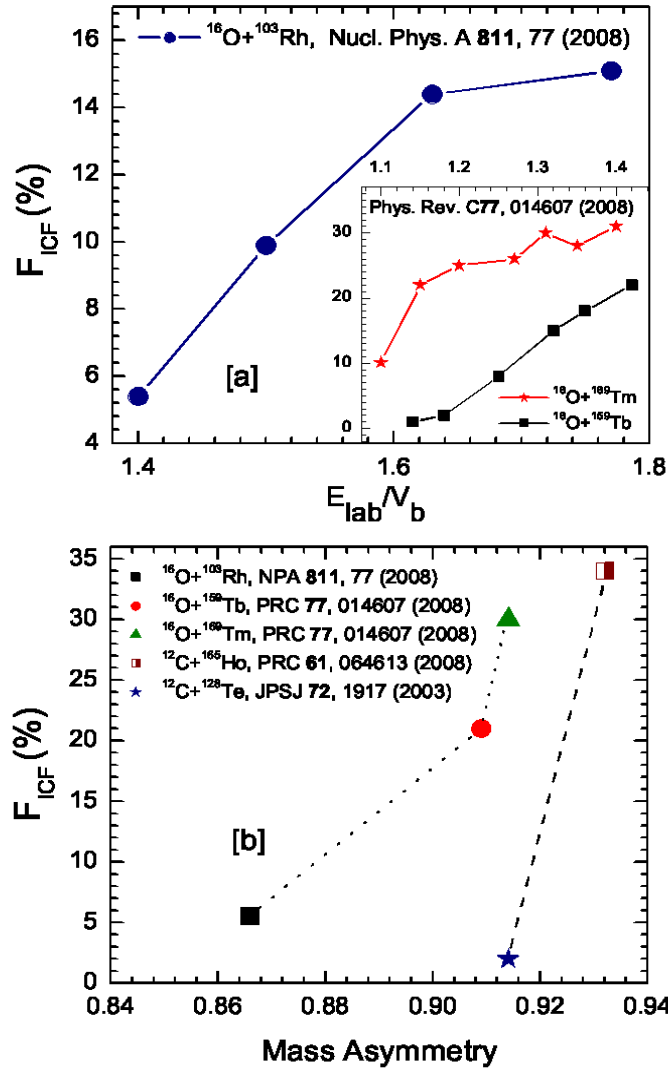


Fig. 1.5 Showing variation of fractional ICF [22]

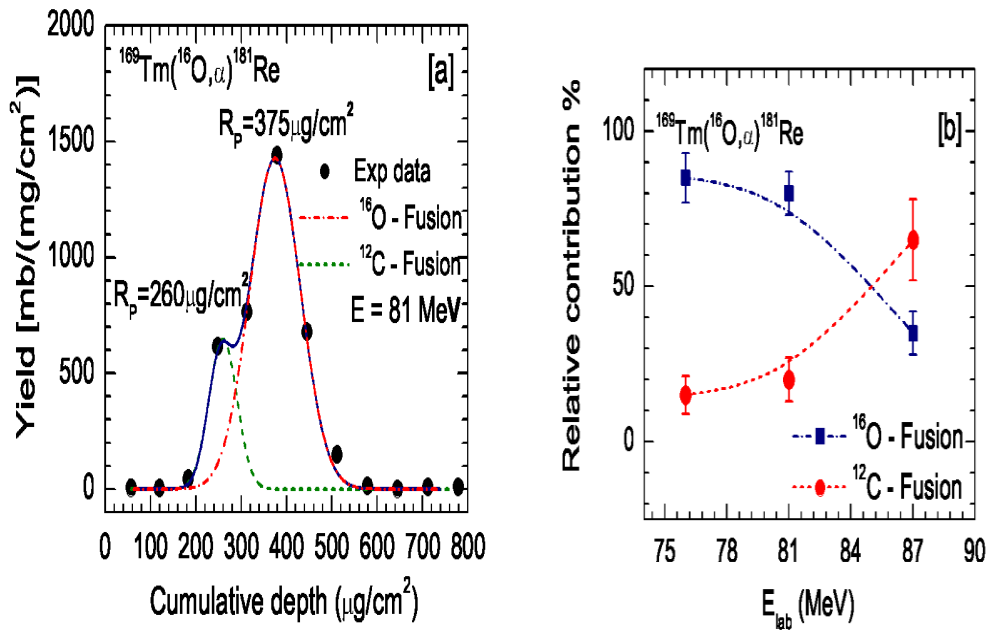


Fig.1.6(a, b) showing CF and ICF results taken from [22]

So far none of the proposed model of ICF give a quantitative estimate of the cross-section of transfer reaction/ ICF reaction in heavy ion reaction and in given energy range. The sum rule model of wilezynski et al [20], which takes into account the transfer/ break-up Q value for the calculation of cross-section for different channels gives a semi-quantitative explanation of NCF process. According to Morgenstern systematics [21], there is a threshold for ICF reaction at $V_1/C = .06 \pm .02$, where V_1 is the velocity of lighter fragment and for the same value, ICF cross-section are more for a mass asymmetric system as compared to symmetric system [22].

1.12 DIC (Deep inelastic collision)

A nuclear reaction in which two nuclei interact strongly, dissipating sizable amounts of energy and exchanging energy and nucleons, while their surfaces overlap for a brief period corresponding to a partial rotation of the intermediate dinuclear complex. Also known as relaxed peak process; strongly damped collision. Heavy ion induced transfer reaction are usually considered to fall into two categories:

- Quasi –elastic(QE) processes on one hand are characterized by small energy transfer with one nucleon transfer reactions being a typical example . These processes are dominant for grazing collisions.

- Deep inelastic collisions(DIC) occur for more central collisions where interaction time is longer and subsequently more energy and particles are exchanged.

QE collision dominate transfer reaction introduced by light heavy ions at energies not too high above barrier while DIC collision are observed mainly in reactions induced by heavier projectiles.

The time-scale of deep inelastic collisions is shorter than the compound nucleus life-time, but long enough for the exchange of significant number of nucleons between the target and the projectile. The DIC product masses are close to the mass of the projectile and target. The kinetic energy spectra of the products formed in deep inelastic collisions extend up to the exit channel Coulomb barrier starting from the beam energy. At very high energy DIC should dominate due to prevalence of coulomb repulsion over nuclear attraction and impossibility of CN formation .In such a case the reaction mechanism depends on n-n potential at constant distance , frictional force at thin region .

The occurrence of DIC in heavy ion reaction has led to development of Dynamical Model, which describes DIC as well as fusion in a unified way. In this model, two heavy ion fuse if there is a pocket in the entrance channel one dimensional interaction potential and a given trajectory (sol. of equation of motion) ends up into the pocket of entrance channel potential. Deep inelastic collisions of heavy ions are characterized by features that are intermediate between those of comparatively simple quasielastic, few-nucleon transfer reactions and those of highly complex compound-nucleus reactions. These deep inelastic or damped collisions often occur for heavy-ion reactions at center-of-mass energies less than 5 MeV per nucleon above the Coulomb barrier. During the brief encounter of the two nuclei, large amounts of kinetic energy of radial and orbital motion can be dissipated. On separation, the final total kinetic energies of the two reaction fragments can be well below those corresponding to the Coulomb repulsion of spheres, indicating that the fragments are highly deformed in the exit channel, as is known to be the case for fission fragments. With the discovery of the deep-inelastic scattering process, two new important aspects of nuclear dynamics were brought into play, namely the time scale and large angular momenta, both of which are associated with the angular velocity of the system.

1.13 Quasi- Fission

The term quasi-fission refers to fully damped processes with a substantial net mass transfer between the two interacting nuclei. Such processes are distinct from complete fusion-fission processes by failing to produce a completely fused system inside the fission barrier. In the fusion reactions involving deformed nuclei the quasi-fission and fusion-fission are in competition. In the quasi-fission process, incoming nuclei in a reaction do not lose its identity during the formation of CN and as a result such a non-equilibrated CN decays into

fragments which are nearly the same as in the entrance channel i.e. projectile and target like fragments. Several experimental studies show that the collision with tip to tip of deformed projectile-target nuclei lead to quasi-fission and the side collisions results in fusion-fission [23],[24]. The terms like gentle fusion and hugging fusion have been coined theoretically [25], which correspond to typical shapes (prolate, oblate and higher multipoles) of deformed nuclei along with their relative orientations. In the quasi fission process one finds large mass rearrangements between the interacting heavy ions occurring on a short time scale. The two nuclei may initially be captured by the nuclear potential, rather than fusing, and they almost always separate after transfer of mass to the lighter nucleus. More recently, the discovery of quasi-fission conceptually bridges between the deep-inelastic scattering processes, for which the energy dissipation is the main aspect, the reaction partners get into close contact to exchange many particles without altering their average mass and charge and the compound fission processes, where the dissipation of energy is complete. Nucleon transfer between the nuclei in a DNS (dinuclear system) is statistical in nature , and there is a possibility that the system may form a compound nucleus.

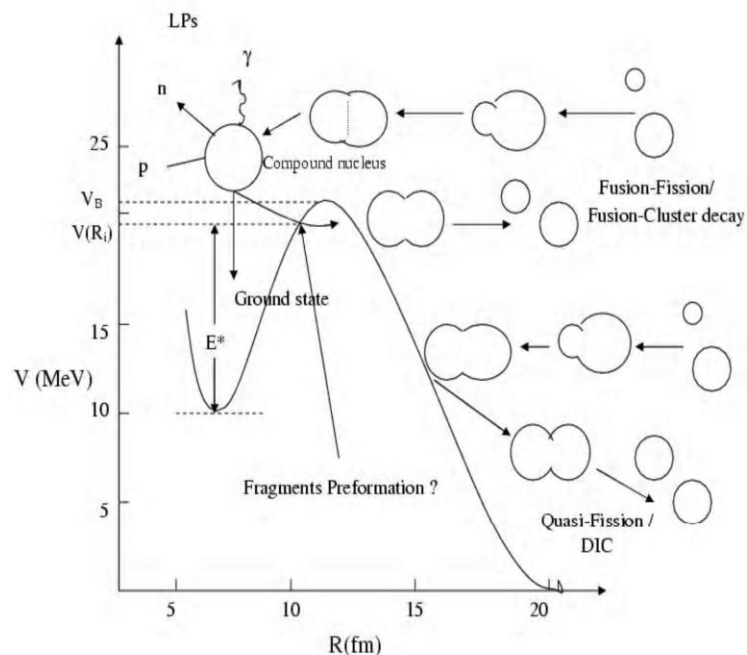


Fig. 1.7 Schematic diagram for dynamics of the colliding nuclei playing around Coulomb as well as nuclear interaction potential [23].

An alternative to that process is the break-up of the system into two fragments quasi-fission. The experimental signatures of this process are the large widths of mass distributions and enhanced angular anisotropy, incompatible with compound nucleus. Fission can inhibit fusion by many orders of magnitude.

Understanding this inhibition may hold the key to forming more super-heavy elements.

1.14 Quasi Fission and Fusion

They have the common property to be described as an evolution of the DNS (dinuclear system) which is formed in the entrance channel during the capture stage of the reaction, after dissipation of the kinetic energy of the collision. One can assume that the decay of the DNS which evolves in mass asymmetry coordinate predestines the charge and mass distributions of the quasi fission products. With the quasi-fission process, we have the opportunity to study the nuclear dynamics in terms of the interplay between reaction time, energy dissipation, and angular momentum, as well as the relations to the complete fusion- fission and deep-inelastic scattering processes. For system with large coulomb repulsion in the entrance channel(symmetrical system) DIC has been reported as major non-compound nucleus channel .Where as for system with higher entrance channel mass asymmetry, ICF has been reported to be dominant non-compound nucleus channel. In such system DIC has been observed at high beam energies.

In the present work we look forward to study the decay of ^{201}Bi formed in $^{20}\text{Ne}+^{181}\text{Ta}$ reaction at $E/A \approx 9$ Mev. In the experimental observation [26] it has been observed that there is a significant contribution of ICF in this nuclear system and ER data and fission data is available. It might be of interest to apply the Dynamical Cluster Decay model on this nuclear system at reported energy to understand the decay mechanism of ^{201}Bi formed in Ne induced reaction. The details of the model are given in chapter 2 and the DCM results are presented in chapter 3.

References

- [1] N.Bohr and J.Wheeler,Phys.Rev.Lett.52,990(1984).
- [2] V. S. Ramamurthy and S. S. Kapoor, Phys. Rev. Lett. **54**, 178 (1985).
- [3] J R Birkelund and J R Huizenga, Ann. Rev. Nucl. Part. Sci. 33, 265 s(1983)
- [4] C Ng^o, Progress in particle and nuclear physics edited by A Faessler (Pergamon Oxford, 1985) vol. 16, p. 139
- [5] B.B. Singh, M.K. Sharma, R.K. Gupta,Phys.Rev. C 77, 054613 (2008)
- [6] R.Gupta, in proceedings of the 5th International Conference on Nuclear Research Mechanics, Varenna, 1988, edited by E. gladioli , (Ricerca Scientifica ed Educazione Permanente ,Milano, 1988),p.416.
- [7] S.S. Malik and R.K.Gupta, Phys.Rev.C 39, 1992(1989)

- [8] R.K.Gupta, W.Scheid, and W.Greiner, *J.Phys.G:Nucl. Part. Phys.* 17, 1731(1991).
- [9] S. Kumar and R.K.Gupta, *Phys.Rev. C* 49, 1922(1994).
- [10] R.K.Gupta and W. Greiner *Int. J. Mod. Phys. E* 3, 335 (1994, Suppl.).
- [11] S. Kumar and R.K.Gupta, *Phys. Rev. C* 55, 218 (1997).
- [12] R.K. Gupta, in *Heavy Elements and Related New Phenomena*, edited by W.Greiner and R.K Gupta (World Scientific Singapore) Vol.II ,p.730
- [13] S.K and R.K Gupta ,*DAE nucl.Phys.(Sambalpur)* 52,365(2007).
- [14] Suparna Sodaye, B S Tomar and A Goswami Vol. 66, No. 6 (2006).
- [15] Yu. Ts. Oganessian, *Heavy Elements and Related New Phenomena*, edited by W.Greiner and R.K Gupta, World Scientific, Singapore, P. 43, (1999).
- [16] H. Ikezoe, S. Mitsuoka, K. Nishio, K. Satou, and I. Nishinaka, *J. Nucl. and Radiochemical Sciences*, 3, 39 (2002).
- [17] A.C.Berrimen et al, *Nature* 413 (2001) 144.
- [18] V.S. Ramanurthy et al , *phys. Rev.Lett.*65 (1990) 25.
- [19] K. Surendra Babu, R. Tripathi, K. Sudarshan, S. K.Sharma, , S..Sodaye ,A. V. R. Reddy A. Goswami, (samhalpur) (NP07), 2007.
- [20] J Wilczynski, K Siwek-Wilczynska, J Van Driel, S Gongrijp, D C J M Hageman, R V F Janssens, , *Nucl. Phys.* A373,109 (1982).
- [21] H Morgenstern, W Bohne, W Galster, K Grabisch and A Kyanowski, *Phys. Rev. Lett* 52, 1104 (1984).
- [22] S pushpendra P. Singh,a, Abhishek Yadav, Devendra P. Singh, Unnati Gupta, M. K. Sharma, K. S. Golda, Rakesh Kumar, R. P. Singh, S. Muralithar, B. P. Singh, R. K. Bhowmik, and R. Prasad *EDP Sciences*(2010).
- [23]K. Nishio, H. Ikezoe, S. Mitsuoka and K. Satou, and S.C. Jeong, *Phys. Rev.C*

[24] D.J Hinde, M. Dasgupta, J.R. Leigh, J.P Lestone, J.C. Mein, C.R. Morton, J.O.Newton, and H. Timmers, Phys. Rev. Lett. 74, 1295 (1995). 63,044610 (2001).

[25] A. Iwamoto, P. Moller, J.R. Nix, and H. Sogawa, Nucl. Phys. A596, 329-354 (1996).

[26] R.Tripathi,K.Sudarshan, A. Gowswami, R.Guin and V.R.Reddy Rdiochemistry Division, Bhabha Atomic research Centre, Mumbai, India (2006)

Chapter - 2

METHODOLOGY

2.1 An Introduction to DCM

The work presented in this thesis deals with the study of heavy ion reaction dynamics using the Dynamical Cluster-decay Model (DCM). This model is used to study the decay of excited (hot and rotating) compound systems formed in low energy heavy ion reactions, including the deformations and orientations degrees of freedom for reactants/products. Note that DCM is a reformulation of PCM for compound nuclei (CN). Both PCM and DCM originate from the Quantum Mechanical Fragmentation Theory, (QMFT) which, in binary fragmentation, uses a collective mass transfer processes. This model gives method of calculating the fragmentation potentials. Collective potentials and kinetic energy part of the Hamiltonian are discussed, together with the solution of the stationary Schrodinger wave equation. In DCM, decay of excited compound nuclei is studied as a collective clusterization process for emissions of the LPs, as well as the IMFs and HMFs, in contrast to the statistical models in which each type of emission is treated on different footing. Another advantage of using the DCM is that the structure effect of CN is also included via the preformation of the fragments with relative probabilities, before penetrating the interaction barrier, a useful information which is missing in the statistical fission models.

The DCM, worked out in terms of the collective coordinates of mass asymmetry $\eta = \frac{A_1 - A_2}{A_1 + A_2}$ and relative separation R respectively gives the nucleon-division between the outgoing fragments, and the transfer of kinetic energy of incident channel (E_{cm}) to internal excitation (total excitation or total kinetic energy, TXE or TKE) of the outgoing channel. This energy transfer process can be calculated with the help of equation

$$E_{CN}^* = E_{c.m} + Q_{in} = IQ_{out} + TKE(T) + TXE(T) \quad (2.1)$$

The CN excitation E_{CN}^* is related to temperature T (in MeV) and is given by

$$E_{CN}^* = \frac{1}{9}AT^2 - T(Mev)$$

DCM defines the decay cross section, in terms of partial waves using the decoupled approximation to R and η -motions [1]-[3] as

$$k = \sqrt{\frac{(2\mu E_{c.m.})}{\hbar^2}}; \sigma = \sum_{l=0}^{l_c} \sigma_l = \frac{\pi}{k^2} \sum_{l=0}^{l_c} (2l+1) P_o P \quad (2.2)$$

Where P_o , the preformation probability refers to η -motion and P, the penetrability to the R-motion. The structure information of the CN enters the model via preformation probability P_o (also known as spectroscopic factor) of the fragments given by the solution of stationary Schrödinger equation in η at the fixed $R=R_a$,

$$\left\{ -\frac{\hbar^2}{2\sqrt{B_{\eta\eta}}} \frac{\partial}{\partial \eta} \frac{1}{\sqrt{B_{\eta\eta}}} \frac{\partial}{\partial \eta} + V_R(\eta, T) \right\} \psi^\nu(\eta) = E^\nu \psi^\nu(\eta) \quad (2.3)$$

with $\nu = 0, 1, 2, 3, \dots$ referring to the ground state and excited state solution. R_a is the first turning point of the penetrability path shown in figure 2.1 for the different l -values. The potential $V(R_a)$ acts like an effective Q-value, Q_{eff} , for the decay of the hot CN at temperature T, to two exit-channel fragments observed (T=0), defined by

$$\begin{aligned} Q_{eff}(T) &= B(T) - [B_L(T=0) + B_H(T=0)] \\ &= TKE(T) = V(R_a(T)) \end{aligned} \quad (2.4)$$

with B's as the respective binding energies.

The above defined decay of a hot CN into two cold (T=0) fragments, via Eq.(2.4), could apparently be achieved only by emitting some light particle(s) (LPs), like n, p, α , or γ -rays of energy. By defining $Q_{eff}(T)$ as in Eq. (2.4), in this model we treat the LP emission at par with the heavy fragments, called intermediate mass fragments (IMFs) emission.

Thus, in this model a non-statistical dynamical treatment is attempted for not only the emission of IMFs but also of multiple LPs, understood so-far only as the statistically evaporated particles in a CN emission. It may be reminded here that the statistical model (CN emission) interpretation of IMFs is not as good as it is for the LP production [4-9].

2.2 The Scattering Potential $V(R)$

For a fixed η i.e for a given target projectile ($A_1;A_2$) combination, the scattering potential $V(R)$ in Eq. (2.3) is defined as the sum of the temperature, deformations and orientations dependent Coulomb potential, proximity potential and angular momentum dependent potential, i.e.

$$V(R, T, \ell) = V_c(Z_i, \beta_{\lambda_i}, \theta_i, T) + V_p(A_i, \beta_{\lambda_i}, \theta_i, T) + V_l(R, A_i, \beta_{\lambda_i}, \theta_i, T)$$

For spherical-plus-deformed nuclear collisions, only one orientation angle θ is enough, referring to the rotationally-symmetric deformed nucleus. $\Phi=0^\circ$ for coplanar nuclei. For the decay of the hot compound nucleus, we use the postulate of first turning point

$$R_a = R_t + \Delta R(T) \quad \text{Where} \quad R_t = R_1 + R_2 \quad (2.5)$$

$\Delta R(T)$ is the neck length parameter that assimilates the neck formation effects. This method is introducing a neck length parameter similar to that used in scission point [4] and saddle point [5],[6] statistical fission model. The R_i are radius vectors which are also made temperature dependent can be calculated as

$$R_i(\alpha_i) = R_{0i} \left[1 + \sum_{\lambda} \beta_{\lambda i} Y_{\lambda}^{(0)}(\alpha_i) \right] \quad (2.6)$$

$$\text{With} \quad R_{0i}(T) = 1.28 A_i^{1/3} - 0.76 + 0.8 A_i^{-1/3} \times (1 + 0.0007 T^2), \quad (2.7)$$

In terms of $Q_{\text{eff}}(T)$, the second turning R_b satisfies (see Fig. 2.1)

$$V(R_a, \ell) = V(R_b, \ell) = Q_{\text{eff}}(T, \ell) = \text{TKE}(T). \quad (2.8)$$

With the ℓ -dependence of R_a defined by

$$V(R_a, \ell) = Q_{\text{eff}}(T, \ell = 0), \quad (2.9)$$

which means that the R_a is the same for all ℓ -values, and that $V(R_a, \ell)$ acts like an effective Q-value, $Q_{\text{eff}}(T, \ell)$, given by the total kinetic energy TKE(T). Then, using (2.8), $R_b(\ell)$ is given by the ℓ -dependent scattering potentials, at fixed T.

Such a potential is illustrated in Fig.2.1 $^{20}\text{Ne} + ^{181}\text{Ta} \rightarrow ^{201}\text{Bi}$, at $\ell = 0$ value. The second turning point R_b is marked for the $\ell = 0\hbar$ case of $R_a = R_t + \Delta R(T)$. The decay path for the ℓ -values begins at $R = R_a$.

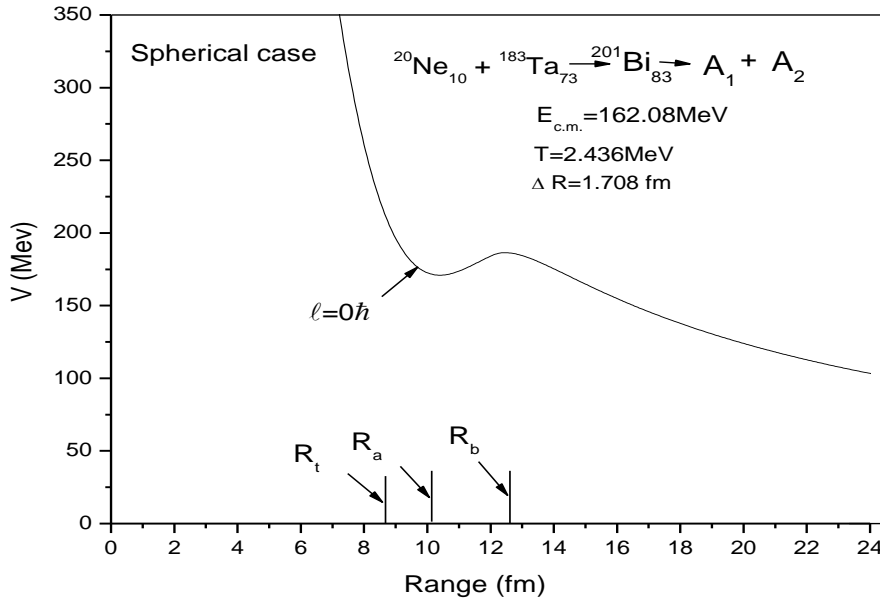


Fig.2.1. Scattering Plot for $^{20}\text{Ne} + ^{181}\text{Ta} \rightarrow ^{201}\text{Bi}$ reaction

2.3 The Fragmentation potential $V(\eta)$

The collective potential energy or the fragmentation potential can be given by $V(\eta, R)$

$$V = \sum_{i=1}^2 B_i(A_i, Z_i, \beta\lambda_i) + V_c(R, Z_i, \beta\lambda_i, \theta_i, \varphi) + V_p(R, A_i, \beta\lambda_i, \theta_i, \varphi) + V_i(R, A_i, \beta\lambda_i, \theta_i, \varphi)$$

(2.10)

The fragmentation potential $V(\eta)$, appearing in equation (2.10) is calculated at a fixed distance $R = R_1 + R_2 + \delta R$ for consideration of deformed and oriented reaction product. Here $\lambda=2,3,4\dots$ and α_i is an angle that the radius vector R_i of the colliding nuclei makes with the symmetry axis.

2.4 The Proximity Potential for deformed, oriented and coplanar nuclei

When two surfaces approach each other within a small distance of less than $\sim 2\text{fm}$, comparable with the surface thickness of interacting nuclei, or when a nucleus is at the verge of dividing into two fragments, then the two surfaces actually face each other across a small gap or crevice. In both cases, the surface energy term alone could not give rise to the strong attraction that is observed when the two surfaces are brought in close proximity. Such additional attractive forces are called proximity forces and the additional potential due to these forces is called the nuclear proximity potential.

Blocki et al. [10] have reanalyzed and extended a theorem, originally due to Deryagin [11], according to which the force between two gently curved surfaces in close proximity is proportional to the interaction potential per unit area between the two flat surfaces. The original expression of Blocki based on the pocket formula was for spherical nuclei, and is given as

$$V_P(s_0) = 4\pi \bar{R} \gamma b \Phi(s_0). \quad (2.11)$$

$\Phi(s_0)$ is the universal function, independent of the shapes of nuclei or the geometry of nuclear system, but depends on the minimum separation distance

$$\Phi(s_0) = \begin{cases} -1/2(s_0 - 2.54)^2 - (s_0 - 2.54)^3 \\ -3.437 \exp(-s_0/0.75) \end{cases} \quad (2.12)$$

respectively, for $s_0 \leq 1.2511$ and $s_0 \geq 1.2511$. Here, s_0 is defined in units of b , i.e. s_0 is s_0/b . This function is defined for negative (the overlap region), zero (touching configuration) and positive values of s_0 . For a fixed R , the minimum distance s_0 for spherical nuclei is defined as

$$s_0 = R - R_1 - R_2 \quad (2.13)$$

where $R = 1.07A_i^{1/3}$ ($i=1,2$). b is the diffuseness of the nuclear surface given by

$$b = [\pi/2\sqrt{3\ln 9}]_{t_{10-90}} \quad (2.14)$$

where t_{10-90} is the thickness of the surface in which the density profile changes from 90% to 10%. The value of $b \sim 1$ fm. The γ is the specific nuclear surface tension given by

$$\gamma = 0.9517[1 - 1.7826(N-Z/A)^2] \text{ Mev fm}^{-2} \quad (2.15)$$

\bar{R} is the mean curvature radius of the reaction partners, characterizing the gap, which for spherical nuclei is given by

$$\bar{R} = R_1 R_2 / R_1 + R_2 \quad (2.16)$$

2.5 The Coulomb potential

Coulomb potential describes the force of repulsion between two interacting nuclei due to their charges. It acts along the line joining the two nuclei. The Coulomb potential for two interacting spherical nuclei is given as

$$V_c = Z_1 Z_2 e^2 / R \quad (2.17)$$

For interacting deformed and oriented nuclei, different authors [12]-[16] have derived it differently. In this thesis work, we have started with Coulomb potential of Wong [15], given for two non-overlapping charge distributions, having quadrupole deformations only, i.e.,

$$V_c = \frac{Z_1 Z_2 e^2}{R} + \left(\frac{9}{20\pi}\right)^{1/2} \left(\frac{Z_1 Z_2 e^2}{R^3}\right) \sum_{i=1}^2 R_i^2(\alpha_i) \beta_{2i} P_2(\cos\theta_i) \\ + \left(\frac{3}{7\pi}\right) \left(\frac{Z_1 Z_2 e^2}{R^3}\right) \sum_{i=1}^2 R_i^2(\alpha_i) [\beta_{2i} P_2(\cos\theta_i)]^2$$

In this expression, the quadrupole-quadrupole interaction term, proportional to $\beta_{21}\beta_{22}$, is neglected since it has a short-range character. For nuclei lying in the same plane we have generalized it to include the higher order deformations ($\lambda = 3, 4\dots$), obtaining

$$V_c(Z_i, \beta_{\lambda i}, \theta_i, T) = \frac{Z_1 Z_2 e^2}{R(T)} + 3Z_1 Z_2 e^2 \sum_{\lambda, i=1,2} \frac{R_i^\lambda(d_i, T)}{(2\lambda+1)R(T)^{\lambda+1}} \left[\beta_{\lambda i} + \beta_{\lambda i}^2 Y_\lambda^{(0)}(\theta_i) \right] \quad (2.18)$$

With $Y_\lambda^{(0)}(\Theta_i)$ is the spherical harmonic function.

2.6 Quantum Mechanical Fragmentation Theory

The QMFT [17]-[30] is a unified description of two body channels in both fusion and fission processes. Here the quantum mechanical concept of probability is utilized to investigate the role of shell effects in the fusion, fission . In QMFT, nuclear dynamics is explained by the mass parameters defining the kinetic energy of the system while the static properties of nuclear system are determined by the potential energy surfaces. The QMFT is worked out in terms of the following collective coordinates:

(i) Relative separation coordinate R between the two nuclei or, in general, two fragments(or, equivalently, the length parameter $\lambda=L/2R_0$, with L as the length of the nucleus and R_0 as the radius of an equivalent spherical nucleus).

(ii) Mass and charge fragmentation co-ordinates [17],[18],[19], defined by the mass and charge-asymmetry coordinates as

$$\eta = \frac{A_1 - A_2}{A}; \quad \eta_Z = \frac{Z_1 - Z_2}{Z} \quad (2.19)$$

Similarly, the neutron asymmetry coordinate [20],

$$\eta_N = \frac{N_1 - N_2}{N}, \quad (2.20)$$

can also be used, but it is sufficient to treat only two of them as dynamical co-ordinates since they are related as

$$\eta = \frac{Z}{A}\eta_Z + \frac{N}{A}\eta_N. \quad (2.21)$$

Here $A = A_1 + A_2$, $Z = Z_1 + Z_2$ and $N = N_1 + N_2$, A_i , Z_i and N_i ($i = 1, 2$) are, respectively, the mass number, the charge number and the neutron number of two fragments. A , Z and N are respectively the mass number, charge number and neutron number of the compound system. The limiting values of η are $0 < \eta < 1$, and thus allows a unified description of a few-nucleon or multi-nucleon (a cluster) transfer, a large-mass transfer, the complete fusion ($\eta = 1$) of nuclei and the symmetric ($\eta = 0$), asymmetric and super-asymmetric fission of a nucleus or compound nucleus. The η_Z coordinate gives the associated charge distribution effects.

(iii) The deformation co-ordinates $\beta\lambda_i$ ($\lambda_i = 2, 3, 4, \dots$ and $i = 1, 2$) of the colliding nuclei or fragments.

(iv) The orientation degrees of freedom θ_i ($i = 1, 2$) of the deformed nuclei.

(v) Azimuthal angle Φ between the principal planes of the two colliding nuclei.

(vi) Neck parameter ϵ , defined by the ratio $\epsilon = E_0/E'$ for the interaction region ($R < R_1 + R_2$). R_i ($i = 1, 2$) is the radius of the two nuclei. Here, E_0 is the actual height of the barrier and E' is the fixed barrier of the two center oscillator. $\epsilon = 0$ represents a broad neck formation, whereas $\epsilon = 1$ gives that the neck is fully squeezed in, corresponding to the asymptotic region ($R = R_1 + R_2$).

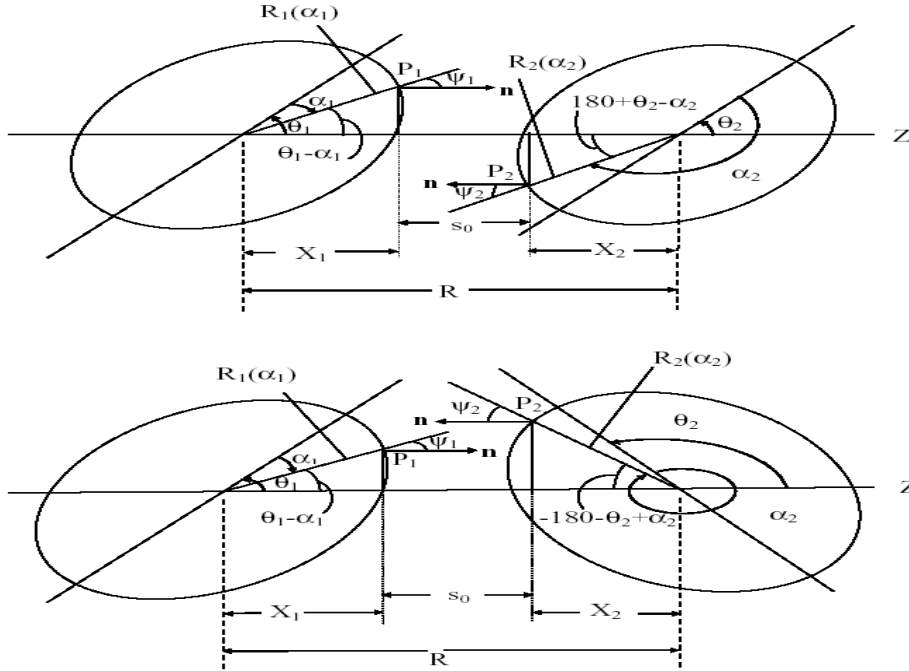


Figure 2.2: Schematic configurations of two (equal/unequal) axially symmetric deformed, oriented nuclei, lying in the same plane and for various Θ_1 and Θ_2 values in the range 0^0 to 180^0 . The Θ 's are measured in anti-clockwise from the colliding axis and the angle α 's in clockwise from the symmetry axis.

2.7 Solution of the Schrödinger Equation and the fragments Preformation Probability (P_0)

Once the Hamiltonian is established, the Schrödinger equation in mass fragmentation co-ordinate η can be solved. On solving numerically, $|\psi^\nu(\eta)|^2$ gives the probability P_0 of finding the mass fragmentation η at a fixed R on the decay path.

$$P_0(A_2) = |\psi^\nu(A_2)|^2 \quad (2.22)$$

For fission studies, like the spontaneous fission and fission through the barrier, the motion in R at the saddle point is adiabatically slow as compared to the η motion. Therefore, the potential is minimized in the neck and deformation coordinates β_1 and β_2 at each R and η values. Starting from the nuclear ground state in spontaneous fission or cluster decay, and to have complete adiabaticity, only the lowest vibrational state $\nu = 0$ is occupied. Then, the mass (or charge)

distribution yield, proportional to the probability $|\psi^{(0)}(\eta)|^2$ or $|\psi^{(0)}(\eta_z)|^2$ of finding a certain mass (or charge) fragmentation η (or ηZ) at a position R on the decay path, when scaled to, say, mass A_2 of one of the fragments ($d\eta = 2/A$) is given by:

$$Y(A_2) = |\psi_R^{(0)}(A_2)|^2 \frac{2}{A} \sqrt{B_{\eta\eta}(A_2)}. \quad (2.23)$$

However, if the system is excited or we allow interaction between various degrees of freedom, higher values of ν would also contribute. These enter via the excitation of higher vibrational states, and through the temperature dependent potential V and masses B_{ij} . The effect of adding temperature on potential V and masses B_{ij} is to reduce the shell effects in them, resulting finally in the liquid drop potential VLDM and smoothed (averaged) masses B_{ij} for the systems to be very hot. Apparently, cold fission means taking both the potential V and masses B_{ij} with full shell effects included in them and hot fission means using the VLDM and smoothed (averaged) masses B_{ij} . Note that we are dealing here with a directly measurable quantity, the mass (or charge) asymmetry, which works dynamically as mass (or charge) transfer coordinate. Thus, the calculated yields $Y(A_i)$ (or $Y(Z_i)$) are directly comparable with experiments. It may be stressed that there is no free parameter in these calculations. The nuclear shape, once minimized in the neck and deformation coordinates β_1 and β_2 at a given R ($=R_{\text{saddle}}$), remains fixed for both the mass and charge distributions of fission or decay fragments.

2.8 Penetration Probability P :

Penetrability P measures the capability of fragments nucleus to penetrate the potential barrier generalized during compound nucleus formation.

2.9 Assault Frequency ν_0 :

For the cluster decay studies in the following section, another quantity of interest is the assault frequency ν_0 defined as, E_2

$$v_0 = v / R_0 = \sqrt{(2 E_2 / \mu)} / R_0 \quad (2.24)$$

where R_0 is the radius of parent nucleus and $E_2 = 1/2\mu v^2$ is the kinetic energy of the emitted cluster. Since both the emitted cluster and the daughter nucleus are produced in the ground state, the entire positive Q-value is the total kinetic energy ($Q = E_1 + E_2$) available for the decay process, which is shared between two fragments, such that for the emitted cluster

$$E_2 = \left(\frac{A_1}{A}\right)Q \quad (2.25)$$

and, $E_1 = Q - E_2$ is the recoil energy of the daughter nucleus.

References

- [1] R.K. Gupta, R. Kumar, N.K. Dhiman, M. Balasubramiam, W. Scheid, and C.Beck, Phys. Rev. C 68, 014610 (2003).
- [2] M. Balasubramiam, R. Kumar, R.K. Gupta, C. Beck, and W. Scheid, J. Phys.G 29, 2703 (2003); R.K. Gupta, M.K. Sharma and B. Singh, Phys. Rev. C
- [3] R.K. Gupta, M. Balasubramiam, R. Kumar, D. Singh, and C. Beck, Nucl.Phys. A 738, 479c (2004).
- [4] R.K. Gupta, M. Balasubramiam, R. Kumar, D. Singh, C. Beck, and W. Greiner, Phys. Rev. C 71, 014601 (2005).
- [5] B. B. Singh, M. K. Sharma, R. K. Gupta, and W. Greiner, Int. J. Mod. Phys. E 15, 699 (2006).
- [6] R.K. Gupta, M. Balasubramiam, R. Kumar, D. Singh, S. K. Arun and W. Greiner, J. Phys. G: Nucl. Part. Phys. 32, 345 (2006).
- [7] B. B. Singh, M. K. Sharma and R. K. Gupta, Phys. Rev. C 77, 054613 (2008).
- [8] T. Matsuse, C. Beck, R. Nouicer, and D. Mahboub, Phys. Rev. C 55, 1380(1997).
- [9] S.J. Sanders, D.G. Kovar, B.B. Back, C. Beck, D.J. Henderson, R.V.F.Janssens, Phys. Rev. C 40, 2091 (1989t).
- [10] S.J. Sanders, Phys. Rev. C 44, 2676 (1991).

- [11] J. Gomez del Campo, R.L. Auble, J.R. Beene, M.L. Halbert, H.J. Kim, A. D'Onofrio, and J.L. Charvet, Phys. Rev. C 43, 2689 (1991); Phys. Rev. Lett. 61, 290 (1988).
- [12] R.J. Charity, M.A. McMahan, G.J. Wozniak, R.J. McDonald, L. G. Moretto, D.G. Sarantites, L.G. Sobotka, G. Guarino, A. Pantaleo, L. Fiore, A. Gobbi and K.D. Hildenbrand, Nucl. Phys. A 483, 371 (1988).
- [13] C. Beck, R. Nouicer, D. Disdier, G. Duchêne, G. de France, R.M. Freeman, F. Haas, A. Hachem, D. Mahboub, V. Rauch, M. Rousseau, S.J. Sanders, and A. Szanto de Toledo, Phys. Rev. C 63, 014607 (2001).
- [14] J. Blocki, J. Randrup, W. J. Swiatecki, and C. F. Tsang, Ann. Phys. (NY) 105, 427 (1977).
- [15] Deryagin, Kolloid Z. 69, 155 (1934).
- [16] N. Malhotra and R.K. Gupta, Phys. Rev. C 31, 1179 (1985).
- [17] M Münchow, D Hahn and W Scheid, Nucl. Phys. A 388, 381 (1982).
- [18] M J Rhoades-Brown, V E Oberacker, M Seiwert and W Greiner, Z. Phys. A310, 287 (1983).
- [19] C Y Wong, Phys. Rev. Lett. 31, 766 (1973).
- [20] R Aroumougame and R K Gupta, J. Phys. G: 6, L155 (1980). J. Maruhn and W. Greiner, Phys. Rev. Lett. 32, 548 (1974).
- [21] R.K. Gupta, W. Scheid and W. Greiner, Phys. Rev. Lett. 35, 353 (1975).
- [22] A. Sîandulescu, R.K. Gupta, W. Scheid and W. Greiner, Phys. Lett. 60B, 225 (1976).
- [23] R.K. Gupta, A. Sîandulescu and W. Greiner, Phys. Lett. 67B, 257 (1977); Rev. Roum. Phys. 23, 51 (1978).
- [24] S. Yamaji, W. Scheid, H.J. Fink and W. Greiner, Z. Phys. A 278, 69 (1976).
- [25] S. Yamaji, W. Scheid, H.J. Fink and W. Greiner, J. Phys. G: Nucl. Phys. 2, L189 (1976).

- [26] S. Yamaji, K.H. Ziegenhain, H.J. Fink, W. Greiner and W. Scheid, J. Phys.G: Nucl. Phys. 3, 1283 (1977).
- [27] R.K. Gupta, A. Sîandulescu and W. Greiner, Z. Naturforsch. 32a, 704 (1977).
- [28] R.K. Gupta, C. Pirvulescu, A. Sîandulescu and W. Greiner, Z. Phys. A 283,217 (1977); Sovt. J. Nucl. Phys. 28, 160 (1978).
- [29] R.K. Gupta, Z. Physik. A 281, 159 (1977).
- [30] A. Sîandulescu, H.J. Lustig, J. Hahn, and W. Greiner, J. Phys. G: Nucl. Phys.4, L279 (1978).
- [31] H.J. Lustig, J.A. Maruhn, and W. Greiner, J. Phys. G: Nucl. Phys. 6, L25(1980).
- [32] H.J. Fink and W. Greiner and R.K. Gupta and S. Liran and J.H. Maruhn and W. Scheid and O. Zohni, in Proceedings of Int. Conf. on Reaction between Complex Nuclei, Nashville, 1974, 21, (Amsterdam: North Holland), pages 2.
- [33]R. K. Gupta, IANCAS Bull. (India), 6, 2(1990).

Chapter – 3

RESULTS and DISSCUSIONS

As it has been discussed in chapter–1 that collision between a heavy ion projectile and a target nucleus leads to the formation of compound nucleus (CN) as well as non-compound nucleus (NCN) or in other words it can be said that the formation of CN in such kind of reactions is not the only possibility, instead the reaction products may also have the contribution from NCN channel. Hence it can not be directly concluded that in what manner the final products of a nuclear reaction would be formed. The solution to this problem is not straight forward and hence needs to be handled with care. Measurement of fission products and evaporation residues in general provide a comprehensive picture of the process subsequent to collision between projectile and target nucleus. However a sizeable amount of non-compound nucleus components like Incomplete Fusion (ICF), Deep Inelastic Collision(DIC), Quasi-Fission(QF) etc., is observed more so at higher energies and for asymmetric reaction partners.

In order to investigate various decay mechanisms in $^{20}\text{Ne}_{10} + ^{181}\text{Ta}_{73}$ reaction forming $^{201}\text{Bi}_{83}$ system, the ER, fission and ICF etc., have been measured in a very recent experiment [1] at $E_{\text{Lab}}=180$ Mev It will be of interest to study the decay $^{201}\text{Bi}_{83}$ and investigate the possibility of non compound nucleus contribution from processes as DIC, ICF,QF along with compound nucleus contribution through ER and fission. First of all we convert E_{Lab} into $E_{\text{c.m}}$ as DCM calculations govern the later parameter in calculations. The center of mass energy ($E_{\text{c.m.}}$) corresponding to this lab energy has been calculated through the relation given by

$$E_{\text{c.m.}} = [A_{\text{T}} / (A_{\text{P}} + A_{\text{T}})] * E_{\text{lab}}$$

The center of mass energy obtained from this relation is $E_{\text{c.m.}}=162.08$ MeV for $E_{\text{Lab}}=180$ MeV. Also it may be notified that for the above reaction, energy per nucleon i.e. $E/A \sim 9$ Mev, thus indicating that all the calculation have been done at the low energy, which is the most widely studied energy range in context of nuclear dynamics and related aspects. For system $^{201}\text{Bi}_{83}$, we have calculated cross- sections of the fission product and evaporation residue for both the spherical and deformed cases in order to find the CN as well as NCN nucleus contribution. As it is well known fact that deformations and orientations play significant role in the decay and formation processes of a nuclear system, so we will present the DCM results with deformation effects included in order to draw comparison with experimental observations. However, towards the end we shall show the mass fragmentation and related aspects with spherical choice as well so as to access the amount and effect of deformation in this decay of $^{201}\text{Bi}_{83}$ nuclear system.

The total experimental evaporation residue(ER) cross-section formed via CN is reported to be 92 mb. With the aim of fitting this number (the ER cross-section) through our calculations based on the DCM model we tried to find that neck length parameter (ΔR) value which could nearly fit the experimental data. After trying a number of arbitrary values of ΔR , we found that $\Delta R=1.246$ fm gives a cross-section comparable to the reported data. It is relevant to mention here that ΔR is the only parameter of model. Although it has been taken so as to fit the experimental data but recent investigation of DCM show that this free parameter seems to have a clear dependence on excitation energy of compound nucleus state. Besides this, in very recent findings it has been shown that the neck length parameter accounts for an important aspect of barrier modification for Ni induced reactions [2]-[5].

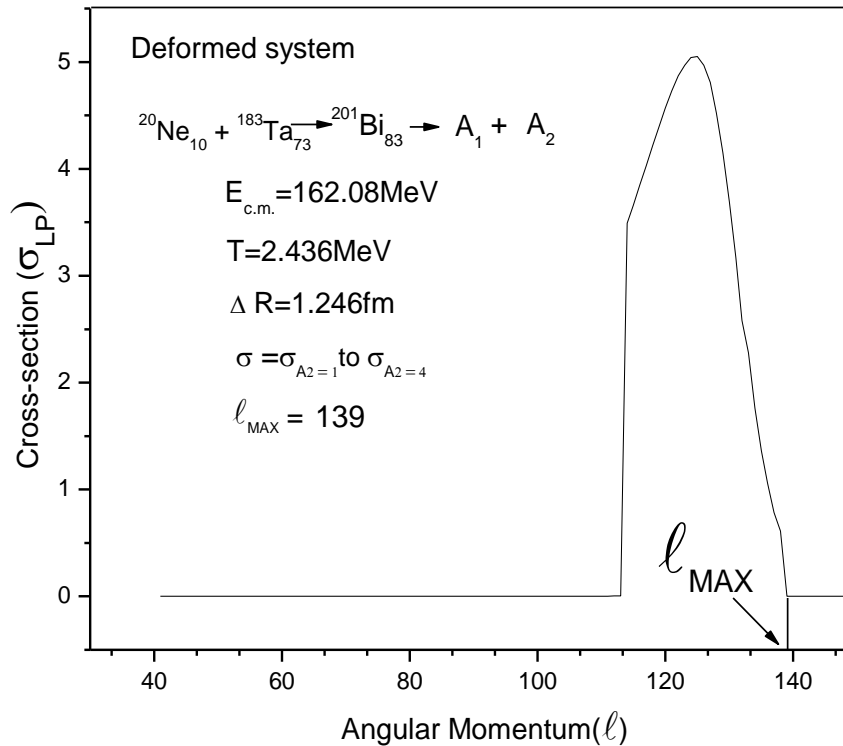


Fig.3.1 Variation of σ_{LP} as a function of angular momentum $\Delta R_{ER}=1.246$ fm.

From σ_{LP} (cross-section of lighter particles) vs ℓ (angular momentum) behavior shown in fig. 3.1 its observed that $\sigma_{LP} \rightarrow 0$ at $\ell=139$. This demonstrates the fact that ℓ_{Max} is decided at a point where lighter particle cross-section become negligibly small. So we take $\ell_{Max} = 139$ at $E_{C.M.}=162.08$ MeV and $\Delta R=1.246$ fm.

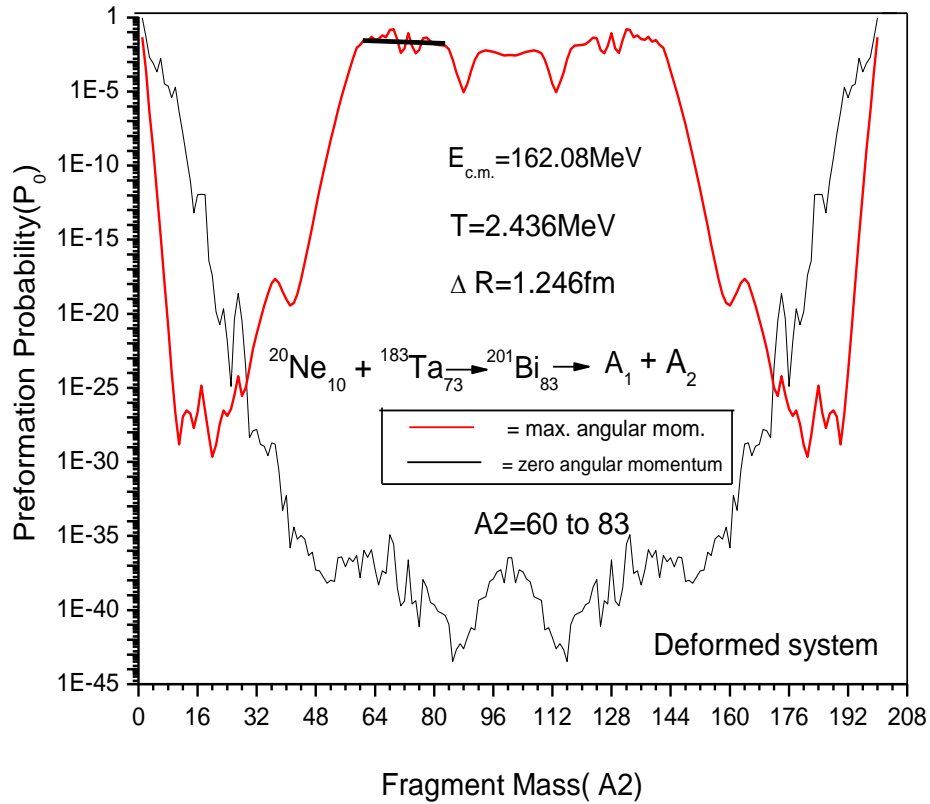


Fig 3.2 Graph for preformation probability at $\Delta R_{ER} = 1.246 \text{ fm}$

Fig 3.2 shows the preformation probability as a function of fragment mass for two extreme cases of angular momentum i.e. $\ell = 0$ and $\ell = \ell_{\max}$. It can be clearly seen from this figure that at $\ell = 0$ light particles are more prominent and fission fragments are largely suppressed. Whereas with increase in ℓ -value particularly at $\ell = \ell_{\max}$ fission fragments start competing with the lighter particles. The fragments in mass range $A_2 = 60-83$ seem to be contributing for fission processes. The fission cross-section corresponding to fragment mass $A_2 = 60-83$ of the fragments is observed to be equal to 290 mb, whereas experimentally reported value of σ_{fission} for this reaction is 486 mb. Hence fore DCM calculations clearly indicate that perhaps some competing process is contributing in total cross-section as reported in experiment [1]. It may be kept in mind that cross-sections are calculated at neck-length parameter $\Delta R = 1.246 \text{ fm}$ which is more significant for ER calculations. Also it is well established that ER and fission processes can occur at different time scales and hence it will be of interest to look out for

maximum allowed ΔR value and check the fission cross-section across that value of neck-length parameter. The maximum allowed value of ΔR is 1.750 fm which has been decided on the basis that concept of penetration across the barrier is not violated.

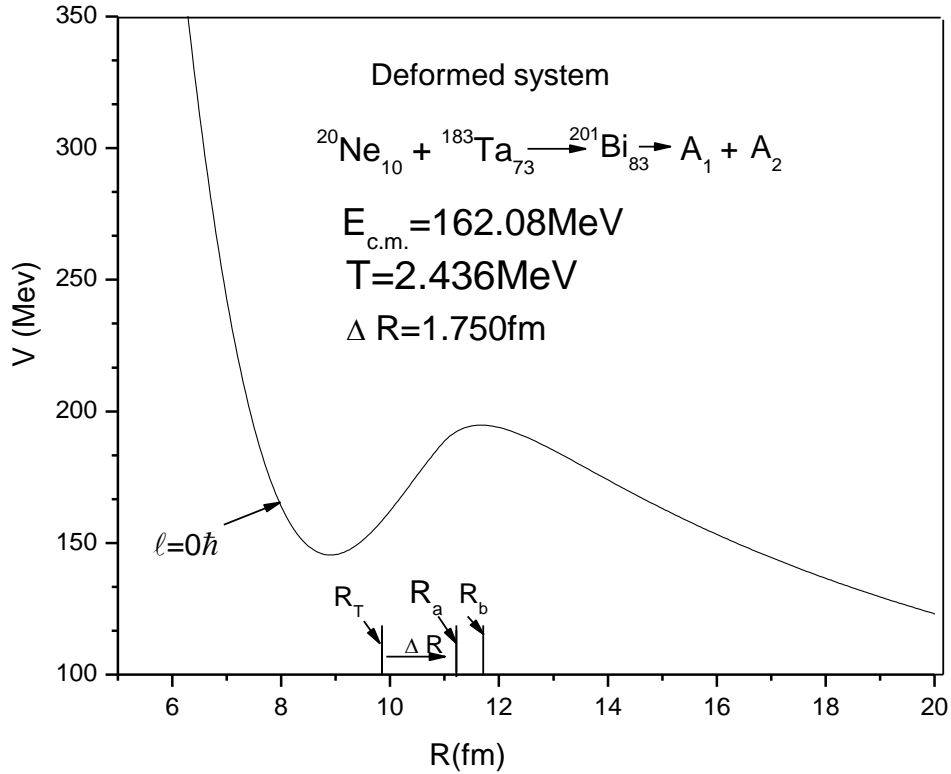


Fig 3.3 Scattering plot for ${}^{20}\text{Ne} + {}^{181}\text{Ta} \longrightarrow \text{Bi}^{201}$ reaction $\Delta R_{\text{fission}} = 1.750 \text{ fm}$

The allowed value of ΔR is checked through the scattering plot which is the variation of total potential $V = V_c + V_f + V_p$ with the nuclear range R shown in fig 3.3. Our calculations reveal that even for maximum allowed ΔR ($\Delta R = 1.750 \text{ fm}$ in this case). The DCM fission cross-section fall short of reported experimental data. It may be noted that a particular value of ΔR is allowed only if $R_a < R_B$. Here $R_a = R_1 + R_2 + \Delta R$ and R_B is the position corresponding to maximum barrier height. Or we can also say that ΔR is allowed if $R_T + \Delta R < R_B$. The maximum angular momentum (ℓ) for this ΔR comes out to be 134 and the dominant fission fragments are almost the same as for the earlier case i.e. from $A_2 = 60$ to 82. The ℓ_{max} value for $\Delta R = 1.750 \text{ fm}$ is shown in fig.3.4.

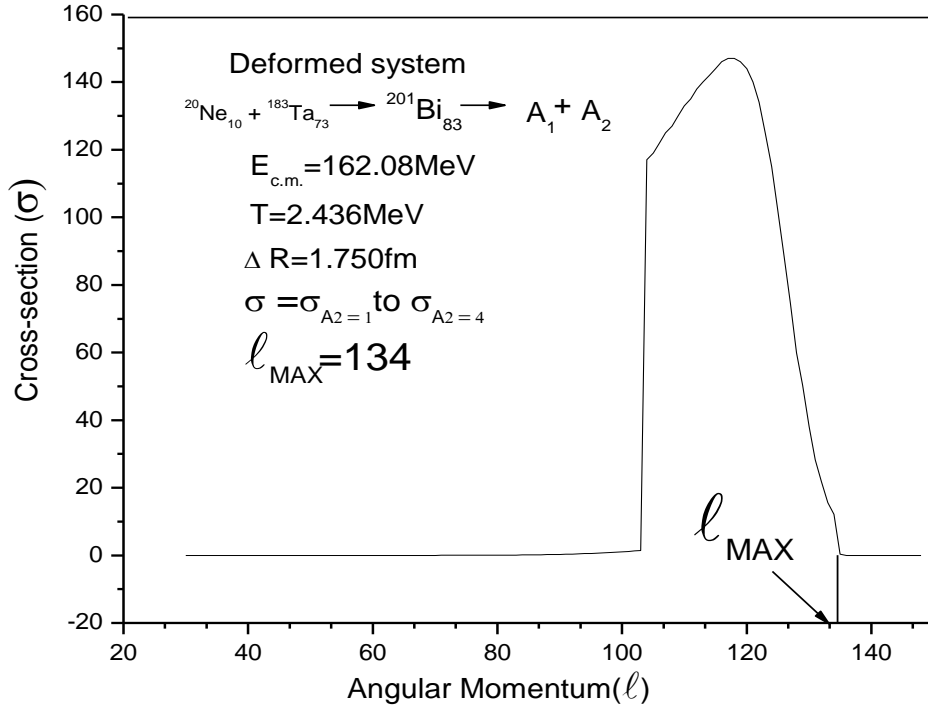


Fig 3.4 Graph for maximum angular momentum for $\Delta R_{\text{fission}}=1.750$ fm

The preformation probability as a function of fragment mass at $\Delta R=1.750$ fm is shown in fig 3.5. The comparison of fig 3.5 with 3.2 tells us that with change in ΔR there is very negligible change in the prominent fission fragments i.e. potential energy surfaces (PES) are almost identical in fig 3.2 and 3.5. However there is significant change in the magnitude of preformation probability. This enhanced preformation probability at $\Delta R=1.750$ fm enables us to increase DCM fission cross-sections upto 468 mb. It is worth noting that this number is still short from referred experimental data by approximately 18 mb. So there seems to be definite scope of some competing Non-Compound Nucleus (NCN) contribution in decay of ^{201}Bi formed in Ne induced reaction at $E_{\text{c.m.}}=162.08$ MeV. Although a significant improvement is seen in σ_{fission} value but still it comes out to be much lower than experimentally reported data. Therefore DCM calculations clearly support the experimental observations that $^{20}\text{Ne}_{10}+^{181}\text{Ta}_{73}\rightarrow^{201}\text{Bi}_{83}\rightarrow A_1+A_2$ reaction seems to have some competing decay process along with ER and fission. Concluding the results from the above calculations at both ΔR 's we can say that at $\Delta R=1.246$ the σ_{ER} matched totally with the experimental value but σ_{fission} did not. Infact, the value for experimental σ_{fission} could not be achieved even at maximum allowed $\Delta R=1.750$ fm.

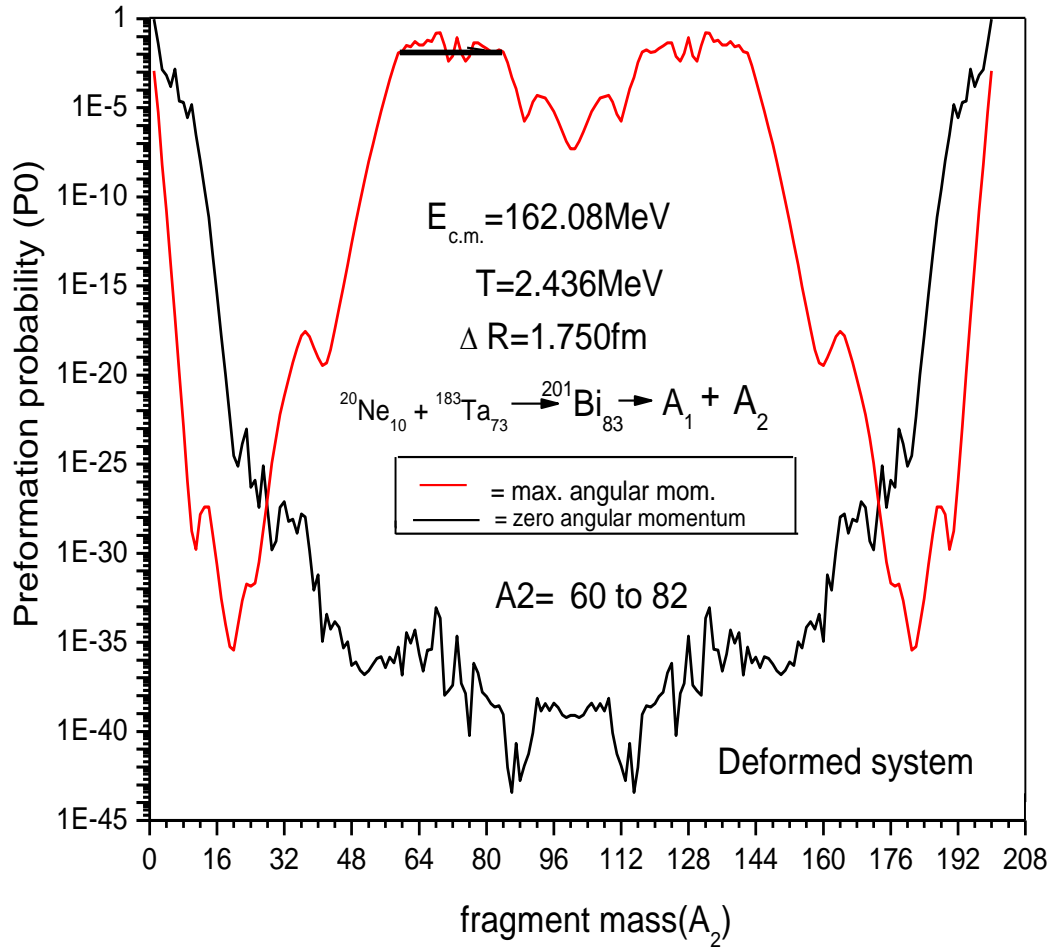


Fig 3.5 Same as fig 3.2, but at $\Delta R_{\text{fission}} = 1.750 \text{ fm}$

Therefore DCM calculations clearly predict the need of competing NCN contribution in decay of ${}^{20}\text{Ne}_{10} + {}^{181}\text{Ta}_{73} \rightarrow {}^{201}\text{Bi}_{83} \rightarrow A_1 + A_2$ reaction. The fragmentation potentials for two selected values of ΔR are shown in figure 3.6. One may clearly see that with change in ΔR from 1.246 fm to 1.750 fm although we find significant change in magnitude of potential, but the behavior of potential energy surfaces remains almost identical. It may be recalled that this change in the magnitude of fragmentation potential is responsible for enhancement in preformation probability reported in fig 3.2 and 3.5. After studying all about deformed system we tried to trace out the changes that could be observed when spherical fragmentation is taken into account. Carrying the foregoing process the value of ΔR at which σ_{ER} could be fitted was at $\Delta R_{\text{ER}} = 1.708 \text{ fm}$ and l_{max} at this ΔR is 131.

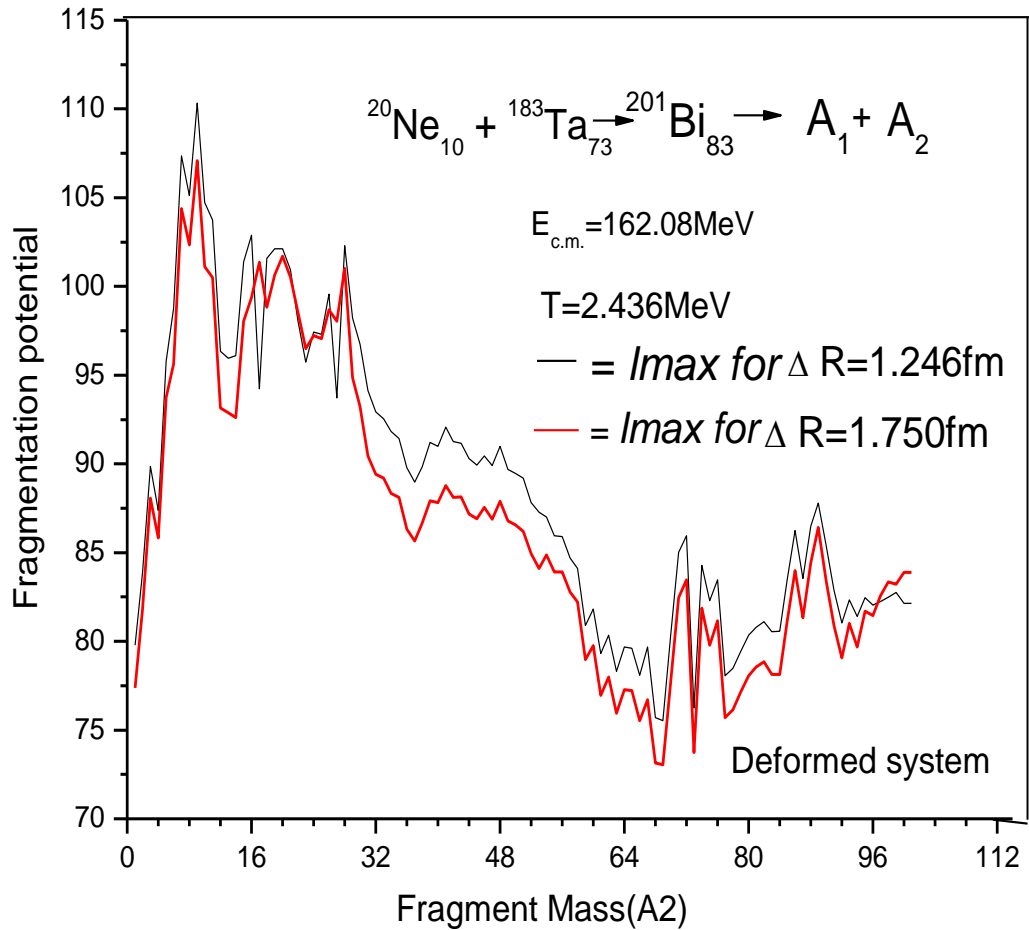


Fig 3.6 Fragmentation potential at I_{Max} for two different ΔR values .

For same ΔR value the σ_{fission} for the fragments given by preformation graph shown in fig. 3.7 viz $A_2 = 88-98$, was found to be 102.3 mb. This made sure that ΔR must be made exceedingly high to fit the required experimental value with spherical consideration. Another point to be noticed in figure 3.7 is that behavior of mass fragmentation changes from asymmetric to near symmetric with exclusion of deformation effects. By comparing fig 3.5 and 3.7, the amount and extent to which deformations are important in the decay of $^{201}\text{Bi}_{83}$ formed in $^{20}\text{Ne}_{10} + ^{181}\text{Ta}_{73}$ reaction, can be easily accessed.

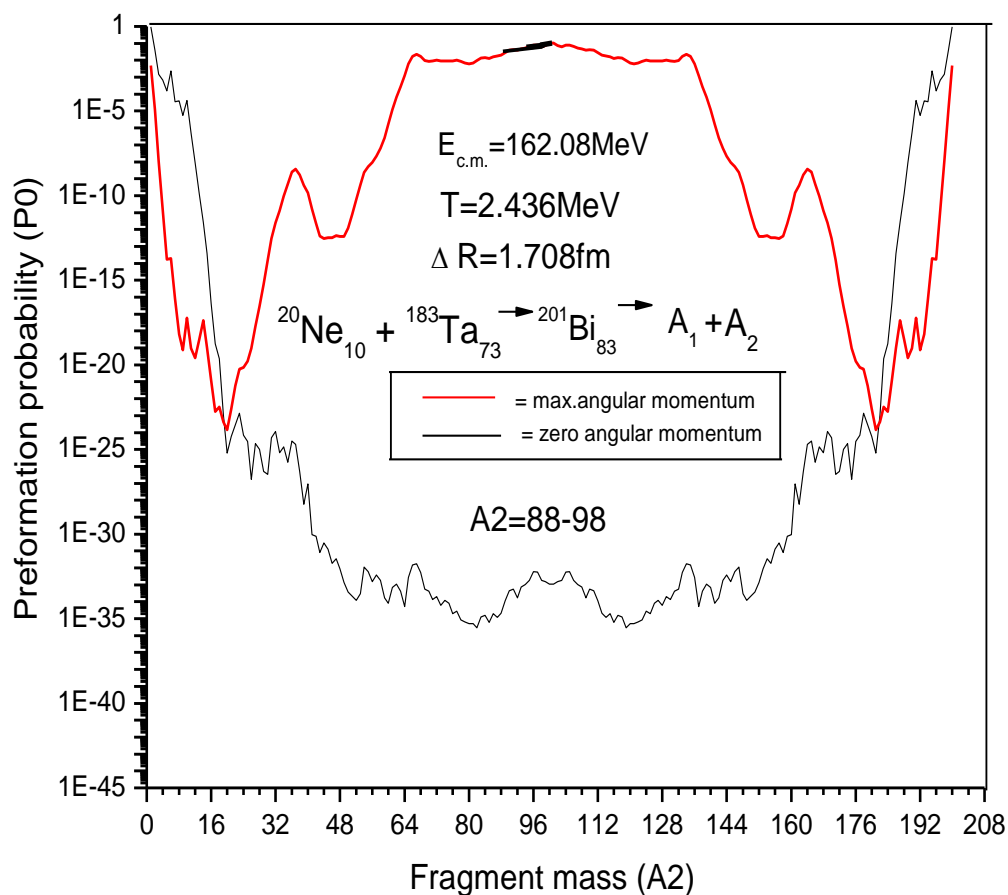


Fig.3.7 Graph for preformation probability for $\Delta R_{ER}=1.708$ fm

We further tried to fit the experimental fission data by taking maximum possible ΔR value i.e. $\Delta R=2$ fm within spherical consideration. It may be noted that $\Delta R > 2$ fm does not make sense in reference to the range of proximity effects. But even for this value of $\Delta R=2$ fm we could not match our results with the experimental data, on the contrary σ_{fission} obtained from these calculations comes out to be 181.5 mb which is extremely small as compared to the deformed choice of fragmentation. However both the choices i.e. spherical and deformed indicate the possibility of non- compound nucleus effects in the decay of ${}^{201}\text{Bi}$ formed in ${}^{20}\text{Ne} + {}^{181}\text{Ta}$ reaction.

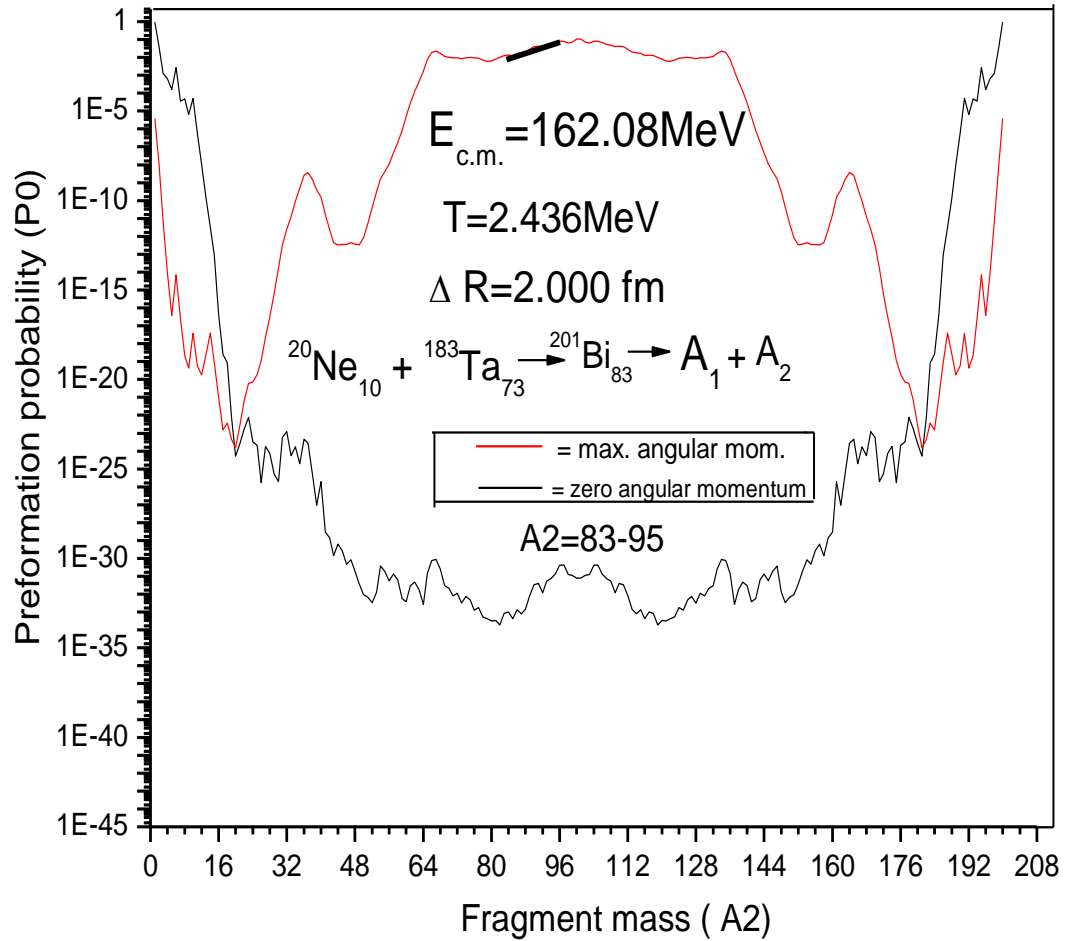


Fig. 3.8 Graph for preformation probability $\Delta R_{\text{fission}} = 2.000 \text{ fm}$

Figure 3.9 shows the scattering plot as a function of nuclear range for deformed and spherical choice of fragmentation. The reported role of deformation described in figures 3.5 and 3.7 can also be accessed from this comparison. Clearly the barrier modification i.e. the change in position and height of potential barrier is reported for the decay of ${}^{201}\text{Bi}$ formed in ${}^{20}\text{Ne}_{10} + {}^{181}\text{Ta}_{73}$ reaction. As the ΔR_{sph} is taken as most probable neck length parameter in reference to experimental data (which is comparable to $\Delta R_{\text{deformed}}$), so there is a definite chance of improvement in this plot which can be done after having idea about the NCN contribution within DCM approach.

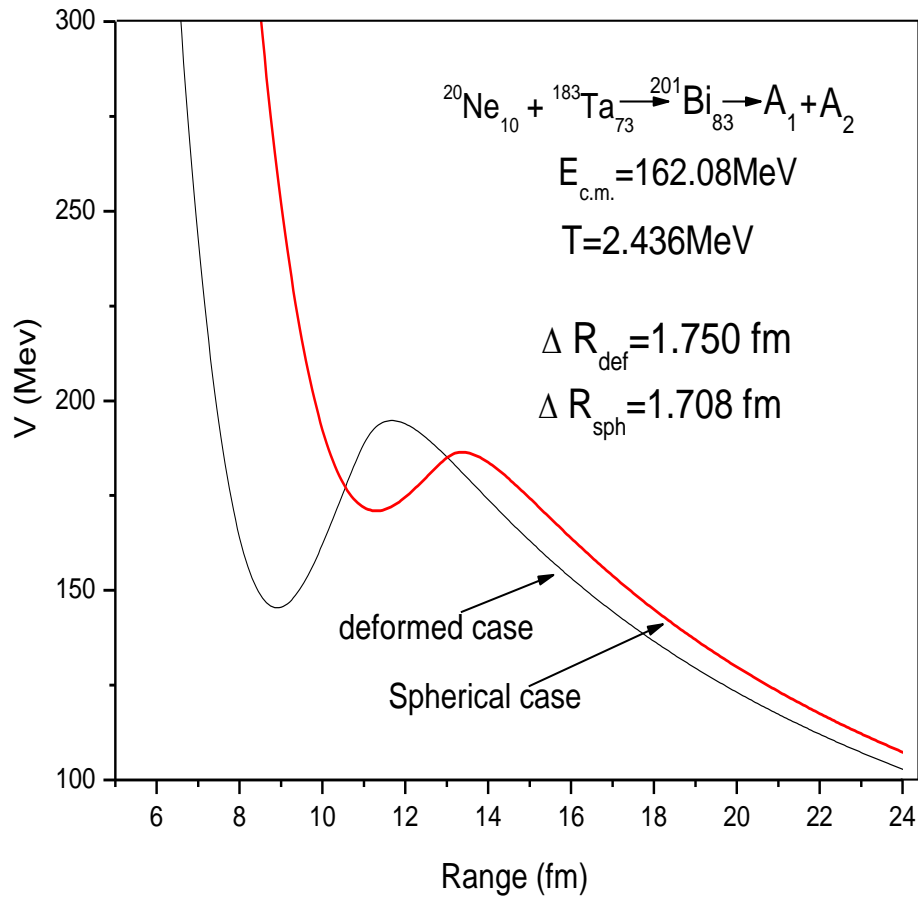


Fig 3.9 Scatering plots for both deformed and spherical fragments.

It is important to note that effects of deformation are quite evident in the decay of ^{201}Bi and the mass fragmentation changes from asymmetric to symmetric for deformed and spherical choice of fragmentation respectively.

Summarizing all these results, we can say that the discrepancy in experimentally observed and the theoretically calculated value of σ_{fission} drew us to the conclusion that apart from compound nucleus contribution there is also a significant non compound nucleus contribution in the decay of ^{201}Bi nucleus. Interestingly NCN component seems relatively weak with inclusion of deformation effects as compared to that for spherical case. It will be of further interest to see the content of NCN in order to find its origin in Incomplete Fusion (ICF), Deep Inelastic Collision (DIC), Quasi-Fission (QF) channel within DCM formation.

References

- [1] R.Tripathi,K.Sudarshan, A. Gowswami, R.Guin and V.R.Reddy Rdiochemistry Division, Bhabha Atomic research Centre, Mumbai, India (2006).
- [2] C.L.Jiang et.al Phys.Rev.C 71 044613 (2005); Phys. Rev. Lett. 93 (2004) 012701.
- [3] S.Misicu and H. Esbensen Phys.Rev.Lett 96, 112701 (2006).
- [4] S.Misicu and H. Esbensen Phys.Rev C 75.034606,(2007).
- [5] S.Kanwar, G.sawhney, M.K.Sharma and R.K. Gupta, Phys.Rev.C- submitted (Ref.C 510218).

